SANDIA REPORT

SAND99–8458
Unlimited Release
Printed March 1999

Structure and Stability of Deflagrations in Porous Energetic Materials

Stephen B. Margolis and Forman A. Williams

Prepared by
Sandia National Laboratories
Albuquerque, New Mexico 87185 and Livermore, California 94550

Sandia is a multiprogram laboratory operated by Sandia Corporation, a Lockheed Martin Company, for the United States Department of Energy under Contract DE-AC04-94AL85000.

Sandia National Laboratories

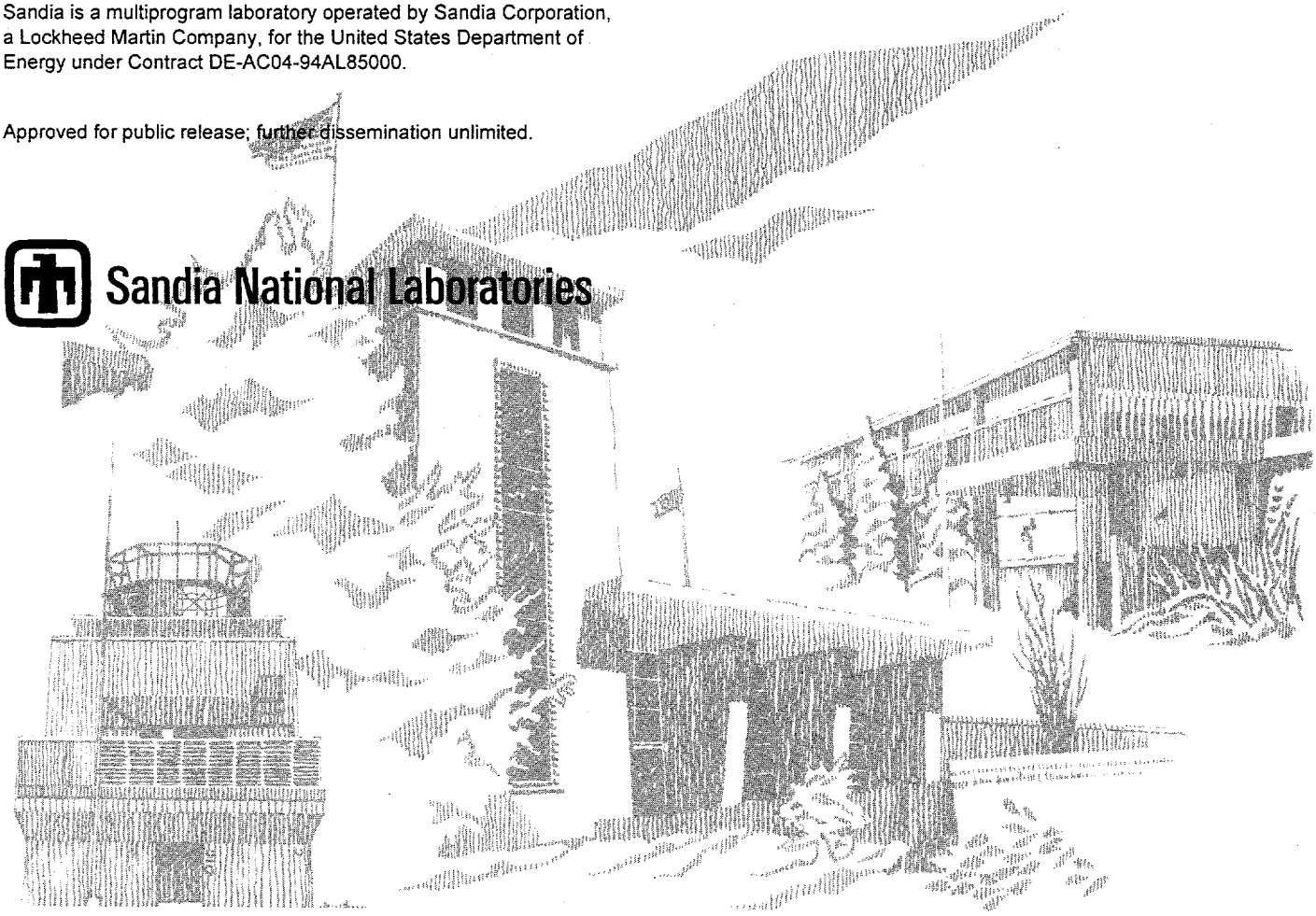

Issued by Sandia National Laboratories, operated for the United States Department of Energy by Sandia Corporation.

Available to DOE and DOE contractors from
Office of Scientific and Technical Information
P.O. Box 62
Oak Ridge, TN 37831

Prices available from (615) 576-8401, FTS 626-8401

Available to the public from
National Technical Information Service
U.S. Department of Commerce
5285 Port Royal Rd
Springfield, VA 22161

NTIS price codes
Printed copy: A03
Microfiche copy: A01

DISCLAIMER

Portions of this document may be illegible in electronic image products. Images are produced from the best available original document.

SAND99-8458
Unlimited Release
Printed March 1999

STRUCTURE AND STABILITY OF DEFLAGRATIONS IN POROUS ENERGETIC MATERIALS*

Stephen B. Margolis†
Sandia National Laboratories, Livermore, California 94551-0969 USA
and
Forman A. Williams‡
University of California at San Diego, La Jolla, California 92093-0411 USA

Abstract

Theoretical two-phase-flow analyses have recently been developed to describe the structure and stability of multi-phase deflagrations in porous energetic materials, in both confined and unconfined geometries. The results of these studies are reviewed, with an emphasis on the fundamental differences that emerge with respect to the two types of geometries. In particular, pressure gradients are usually negligible in unconfined systems, whereas the confined problem is generally characterized by a significant gas-phase pressure difference, or overpressure, between the burned and unburned regions. The latter leads to a strong convective influence on the burning rate arising from the pressure-driven permeation of hot gases into the solid/gas region and the consequent preheating of the unburned material. It is also shown how asymptotic models that are suitable for analyzing stability may be derived based on the largeness of an overall activation-energy parameter. From an analysis of such models, it is shown that the effects of porosity and two-phase flow are generally destabilizing, suggesting that degraded propellants, which exhibit greater porosity than their pristine counterparts, may be more readily subject to combustion instability and nonsteady deflagration.

*Work supported by the United States Department of Energy under Contract DE-AC04-94AL85000.
†Principal Member of Technical Staff, Combustion Research Facility.
‡Professor, Department of Applied Mechanics and Engineering Sciences.

STRUCTURE AND STABILITY OF DEFLAGRATIONS IN POROUS ENERGETIC MATERIALS

I. Introduction

The combustion behavior of porous energetic materials is of increasing interest due to the realization that even supposedly nonporous materials may develop significant porosities over time due either to aging or to other types of degradation that may arise from exposure to abnormal environments. In such materials, two-phase-flow effects are especially significant due to the presence of gas flow relative to the condensed material both within the unburned porous solid as well as in the exothermic liquid/gas layers that typically form on the surfaces of many types propellants, such as nitramines.[1-5] In the presence of confinement, the significance of the convective transport effects due to two-phase flow are enhanced, leading, through gas permeation into the unburned solid, to a preheating of the solid and, consequently, to a strong enhancement of the burning rate relative to the unconfined case. Indeed, this type of preheating associated with gas permeation into the unburned solid is generally associated with the onset of specially identified modes of combustion, such as convective burning (*cf.* Ref. 6 and the additional references therein). However, even in unconfined problems, two-phase-flow effects play an important role, affecting not only fundamental thermodynamic characteristics such as the burned temperature, but also the burning rate and the stability of steady, planar burning.

In the present work, we synthesize and describe the results of several recent analyses that, by means of asymptotic methods, have been successful in predicting the effects of two-phase flow on the structure, burning rate and linear stability of a propagating deflagration wave.[7-12] For the case of a confined or partially confined geometry, a quasi-steady propagation regime can be identified such that in the limit that the pressure difference, or overpressure, between the burned and unburned regions approaches zero, the combustion wave collapses to that corresponding to an unconfined deflagration. Indeed, a sketch of the geometry for the simplified chemistry adopted here is shown in Fig. 1, which indicates an unburned solid/gas region, a melting surface, a liquid-gas region within which is embedded a thin reaction zone in which burning takes place, and finally a burned gaseous product region. The primary difference between the unconfined and confined problems is that in the case of confinement, the direction of gas flow in the unburned region is likely to be negative, resulting in a preheating effect that results in a rapid increase in the burning rate as a function of overpressure. This permeation-enhanced burning is generally referred to, for obvious reasons, as convective burning, and one of the successes of the present model formulation and analysis is the ability to predict the transition from ordinary conduction-controlled burning that is characteristic of unconfined deflagrations to one in which convection plays a significant role.

The model used to investigate the wave structure described above is essentially a simplified version of more general models of two-phase reacting flow (*cf.* Ref. 13). In particular, the model essentially consists of continuity and energy equations for each coexisting phase, a simplified ac-

counting for momentum conservation appropriate for deflagrations, an equation of state for the gas, and an appropriate set of boundary and melting surface conditions. Although it is critical to the focus of our study to allow for velocity differences between coexisting phases, for simplicity we assume good thermal contact and adopt the single-temperature approximation that the temperature at a given spatial location is the same for each phase. Also, in keeping with our goal of focusing on two-phase-flow effects, we deliberately simplify the chemistry by postulating the overall process $R(s) \longrightarrow R(l) \longrightarrow P(g)$, where the first step denotes the melting (assumed to be slightly endothermic) of the solid material, and the second represents a one-step exothermic process in which liquid-phase reactants are directly converted to burned gaseous products. Extensions of the analysis to more complicated global mechanisms have been given,[5,10,11] but such extensions are not critical to the examination of the primary two-phase-flow effects of interest here.

In what follows, we first present the formulation and nondimensional models that will be considered for the analysis of the two types of problems (confined and unconfined) introduced above (Sections II and III). The case of steady (unconfined) or quasi-steady (confined) burning is then considered in order to derive, via asymptotic methods, analytical expressions for the respective planar burning rates and other aspects of the deflagration structure (Sections IV and V). A time-dependent, multidimensional asymptotic model, one in which the reaction zone becomes represented by a reaction sheet, is then derived (Section VI) and used to examine the stability of a basic planar mode of burning (Sections VII and VIII). Finally, the results and indications for future investigations are summarized in the Conclusion (Section IX).

II. Formulation

A sketch of the physical problem is shown in Fig. 1. The unburned porous solid lies generally to the left, and the burned gas products lie to the right. The two are separated by a deflagration wave that generally moves from right to left, converting the former into the latter. These regions (unburned and burned) in turn are bounded on the left and right, respectively, but these boundaries are assumed to be sufficiently far away (relative to the width of the flame region) such that the only significant effect on the combustion wave itself occurs in the case of confinement, where a significant difference develops between the upstream and downstream values of the pressure. In the unconfined problem, the gas flow is unrestricted in the burned region and pressure gradients remain sufficiently small that they may be neglected on the nonacoustic scales of interest here. In the confined case, however, gas flow in the burned region is restricted and hence the continual production of gas via chemical reaction causes the pressure to become greater in the burned region than in the unburned solid. This pressure difference drives at least some of the gas upstream in the direction of the unburned solid, where momentum conservation plays a critical role in reducing the gas velocity far upstream to zero so as to satisfy the ambient conditions there. Depending on the magnitude of the overpressure, the gas velocity in the burned region, on the other hand, may be either positive or negative. Hence, for moderate overpressures, the gas velocity can experience

a turning point within the reaction region where the gaseous products are generated.

The structure of the combustion wave thus consists of a solid/gas preheat region that, for the confined problem, contains a gas-permeation boundary layer in which the pressure rises from its ambient value to its larger (possibly much larger) value in the liquid/gas region, the melting surface that marks the left boundary of a liquid/gas preheat region (and the right boundary of the gas-permeation layer if one exists), the liquid/gas preheat zone, a relatively thin exothermic reaction layer in which chemical reaction occurs, and the burned gaseous region that extends to the right boundary. In the limit that the activation energy of reaction is large, the reaction zone asymptotically becomes a propagating surface similar to, but displaced from, the melting surface. In the laboratory-fixed spatial coordinate system $(\tilde{x}_1, \tilde{x}_2, \tilde{x}_3)$, the porous solid extends to $\tilde{x}_3 = -\infty$, where conditions are denoted by the subscript u, and the gas extends to $\tilde{x}_3 = +\infty$, where conditions are identified by the subscript b. The deflagration generally propagates in the $-\tilde{x}_3$ direction, although, in general, the wave motion is allowed to be both nonsteady and nonplanar. Here and in what follows, a tilde over a symbol (*e.g.*, $\tilde{x}_3$) will denote a dimensional quantity, and the subscripts s, l and g will denote solid, liquid and gas-phase quantities, respectively. A continuum formulation, in which appropriate gas- and condensed-phase volume fractions (α and $1-\alpha$, respectively) multiply the physical variables associated with each phase, will be used to model the physical problem just described.

The governing system of equations that will be considered incorporate a number of assumptions that greatly simplify the analysis without compromising the fundamental two-phase-flow aspects of the problems of interest here. Two of these include restricting the analysis to the single-temperature limit and considering only weakly nonplanar deflagrations. The first implies sufficiently good thermal contact between co-existing phases such that corresponding temperature differences are small, while the latter, which implies that the transverse velocity components are small relative to the component of velocity in the $\tilde{x}_3$-direction, allows the velocity field (for the gas and liquid phases) to be approximated by $\tilde{\mathbf{u}}_{l,g} \sim (0, 0, \tilde{u}_{l,g}(\tilde{x}_1, \tilde{x}_2, \tilde{x}_3, \tilde{t}))$, with the velocity of the solid assumed to be zero. Other assumptions will be indicated as they are introduced. We remark that the single-temperature assumption, which can be readily relaxed by considering the limit of sufficiently large, but finite, rates interphase heat, transfer,[7,14] is quite reasonable for many two-phase-flow problems. In contrast, the corresponding limit of large interphase momentum transfer is not so plausible,[4,7] and thus it is important to retain velocity differences in the model if one wishes to capture true two-phase-flow effects.

Denoting the melting surface that separates the solid/gas and liquid/gas regions by $\tilde{x}_3 = \tilde{x}_m$, and the gas-phase volume fraction by α, continuity in the region $\tilde{x}_3 > \tilde{x}_m$ is expressed separately for the liquid and gas phases, where the latter may be replaced by an overall continuity equation for the two-phase medium. Consequently, we have

$$\frac{\partial}{\partial \tilde{t}}\left[(1-\alpha)\tilde{\rho}_l\right] + \frac{\partial}{\partial \tilde{x}_3}\left[(1-\alpha)\tilde{\rho}_l\tilde{u}_l\right] = -\tilde{A}\tilde{\rho}_l(1-\alpha)\exp\left(-\tilde{E}_l/\tilde{R}^\circ\tilde{T}\right), \quad \tilde{x}_3 > \tilde{x}_m, \tag{1}$$

$$\frac{\partial}{\partial \tilde{t}}\left[(1-\alpha)\tilde{\rho}_l + \alpha\tilde{\rho}_g\right] + \frac{\partial}{\partial \tilde{x}_3}\left[(1-\alpha)\tilde{\rho}_l\tilde{u}_l + \alpha\tilde{\rho}_g\tilde{u}_g\right] = 0\,, \quad \tilde{x}_3 > \tilde{x}_m\,, \tag{2}$$

where $\tilde{\rho}$, $\tilde{u}_l$, $\tilde{T}$ and $\tilde{t}$ denote density, velocity, the single temperature and time, respectively. For simplicity, we will assume a constant value for $\tilde{\rho}_l$, but not for $\tilde{\rho}_g$. In the reaction rate expression, $\tilde{E}_l$ is the overall activation energy, $\tilde{R}^\circ$ is the universal gas constant, and $\tilde{A}$ is the exponential reciprocal-time prefactor which, for simplicity, will be assumed constant. For this type of global kinetic modeling, however, it may be reasonable to assign a pressure, as well as a temperature, dependency to $\tilde{A}$. In the solid/gas region $\tilde{x} < \tilde{x}_m$, we assume for the solid phase a constant density $\tilde{\rho}_s$ and zero velocity ($\tilde{u}_s = 0$), with $\alpha \equiv \alpha_s$ also constant in this region. Gas-phase continuity for $\tilde{x} < \tilde{x}_m$ is thus independent of the solid phase and is given by

$$\frac{\partial \tilde{\rho}_g}{\partial \tilde{t}} + \frac{\partial}{\partial \tilde{x}_3}\left(\tilde{\rho}_g\tilde{u}_g\right) = 0\,, \quad \tilde{x}_3 < \tilde{x}_m\,. \tag{3}$$

Conservation of energy for each phase in the liquid/gas and solid /gas regions is similarly given by separate equations for each coexisting phase, which, as before, may be summed to give an overall energy equation in each region. In the single-temperature limit, however, only the overall energy equations remain and these are given by

$$\begin{aligned}\frac{\partial}{\partial \tilde{t}}\left[\tilde{\rho}_l(1-\alpha)(\tilde{Q}+\tilde{c}_l\tilde{T}) + \tilde{\rho}_g\tilde{c}_g\alpha\tilde{T}\right] + \frac{\partial}{\partial \tilde{x}_3}\left[\tilde{\rho}_l\tilde{u}_l(1-\alpha)(\tilde{Q}+\tilde{c}_l\tilde{T}) + \tilde{\rho}_g\tilde{c}_g\tilde{u}_g\alpha\tilde{T}\right] \\ = \tilde{\nabla}\cdot\left[\tilde{\lambda}_l(1-\alpha)\tilde{\nabla}\tilde{T} + \tilde{\lambda}_g\alpha\tilde{\nabla}\tilde{T}\right] + \alpha\frac{\partial \tilde{p}_g}{\partial \tilde{t}}\,, \quad \tilde{x}_3 > \tilde{x}_m\,,\end{aligned} \tag{4}$$

$$\begin{aligned}\frac{\partial}{\partial \tilde{t}}\left[\tilde{\rho}_s\tilde{c}_s(1-\alpha_s)\tilde{T} + \tilde{\rho}_g\tilde{c}_g\alpha_s\tilde{T}\right] + \frac{\partial}{\partial \tilde{x}_3}\left(\tilde{\rho}_g\tilde{c}_g\tilde{u}_g\alpha_s\tilde{T}\right) \\ = \tilde{\nabla}\cdot\left[\tilde{\lambda}_s(1-\alpha_s)\tilde{\nabla}\tilde{T} + \tilde{\lambda}_g\alpha_s\tilde{\nabla}\tilde{T}\right] + \alpha_s\frac{\partial \tilde{p}_g}{\partial \tilde{t}}\,, \quad \tilde{x}_3 < \tilde{x}_m\,,\end{aligned} \tag{5}$$

where Eq. (1) has been used to eliminate the reaction-rate term in Eq. (4). Here, $\tilde{c}$, $\tilde{\lambda}$ and $\tilde{p}$ denote heat capacity (at constant volume for the liquid, and at constant pressure for the gas, both assumed constant), thermal conductivity and pressure, respectively, and $\tilde{Q}$ is the heat release for the global reaction at temperature $\tilde{T}$. We remark that because of the small Mach number and the small ratio of gas-to-condensed phase densities in the problems to be considered, no terms involving the pressures in the condensed phases appear in these equations. Terms involving $\tilde{p}_g$, however, arise from the contribution to the rate of change of the internal energy of the gas from the sum of the rate of surface work $-\partial(\alpha\tilde{u}_g\tilde{p}_g)/\partial\tilde{x}$ and the rate of volume work $-\tilde{p}_g\partial\alpha/\partial\tilde{t}$ performed by the gas.

Although analogous equations may be written for momentum conservation, we avoid introducing them explicitly by adopting certain simplifying approximations which are often used in these types of problems. In particular, in place of gas-phase momentum, we adopt, depending on the type of problem, either the assumption of constant pressure throughout or Darcy's law (in the solid/gas region). In the latter instance, which provides a convenient formulation when pressure

gradients are not negligible (as in the confined geometry introduced below), it is still reasonable to assume, based on the assumption of small Mach number, that the gas pressure is homogeneous in the liquid/gas region. If it is further assumed that the gas pressure in the burned region varies on a longer time scale than that associated with the flame structure itself (*e.g.*, when the confining boundary is sufficiently remote with respect to the flame), then the upstream and downstream pressures may be regarded as constant in the quasi-static sense. This argument is supported by numerical calculations,[15] which, though based on the assumption of a flame sheet propagating with constant velocity, nonetheless enabled the authors to correctly identify this quasi-steady regime, which they described as a "gas-permeation boundary-layer solution." The latter refers to the fact that the solution is characterized by a relatively thin gas-permeation layer in the solid/gas region, described below in the context of the present model, that arises from the difference, or overpressure, between the upstream and downstream values of the gas pressure. Thus, in place of gas-phase momentum, we adopt either the conditions

$$\tilde{u}_g = -\frac{\tilde{\kappa}(\alpha_s)}{\alpha_s \tilde{\mu}_g}\frac{\partial \tilde{p}_g}{\partial \tilde{x}_3}\,, \quad \tilde{x} < \tilde{x}_m\,; \qquad \tilde{p}_g = \tilde{p}_g^b > \tilde{p}_g^u\,, \quad \tilde{x} > \tilde{x}_m\,, \tag{6a}$$

which is appropriate for the confined problem, or, for the unconfined problem,

$$\tilde{p}_g = \tilde{p}_g^u\,, \quad -\infty < \tilde{x} < +\infty\,. \tag{6b}$$

Here, the first of Eqs. (6a) is the planar approximation of Darcy's law, $\tilde{\mathbf{u}}_g = -\tilde{\kappa}\tilde{\nabla}\tilde{p}_g/(\alpha_s\tilde{\mu}_g)$, implied by the planar representation of the velocity field introduced above. The coefficient $\tilde{\kappa}$ is the permeability of the solid/gas region and $\tilde{\mu}_g$ is the gas-phase viscosity, while the value $\tilde{p}_g^u$ is the specified upstream boundary condition on the gas pressure according to Eq. (9) below. We observe that Eq. (6b) is actually obtainable from Eq. (6a) in the limit $\tilde{\kappa} \to \infty$ (which implies $\tilde{p}_g^b \to p_g^u$), so that in the aforementioned quasi-steady burning regime, the solution to the unconfined problem constitutes a limiting case of the corresponding solution obtained from the more general condition given by Eq. (6a).

The equation of state for the gas is assumed to be ideal, and thus $\tilde{p}_g$ is, in general, coupled to the other field variables through the gas-phase equation of state,

$$\tilde{p}_g = \tilde{\rho}_g \tilde{R}^\circ \tilde{T}/\tilde{W}_g\,, \tag{7}$$

where $\tilde{W}_g$ is the molecular weight of the product gas. Consideration of condensed-phase momentum, on the other hand, leads in principle to an equation for the liquid-phase velocity $\tilde{u}_l$. Based on a previous analysis,[4] a reasonable first approximation is to set the condensed velocity equal the condensed mass burning rate divided by the condensed-phase density. In the present context, this implies that, since $\tilde{u}_s = 0$,

$$\tilde{u}_l = -\frac{\partial \tilde{x}_m}{\partial \tilde{t}}\left(\frac{\tilde{\rho}_s}{\tilde{\rho}_l} - 1\right)\,, \quad \tilde{x}_3 > \tilde{x}_m\,, \tag{8}$$

where $\partial \tilde{x}_m/\partial \tilde{t} < 0$ is the (unknown) propagation velocity of the melting surface. A modification to this expression that introduces a linear dependence of $\tilde{u}_l$ on the gas-phase volume fraction α

that qualitatively takes into account viscous and surface-tension-gradient (Marangoni) effects in the liquid/gas region has been proposed,[4] but in the present work we shall adopt the simpler result given by Eq. (8).

The above equations now constitute a closed set for the variables α, $\tilde{u}_g$, $\tilde{T}$, $\tilde{\rho}_g$ and $\tilde{p}_g$. The problem is thus completely determined once initial and boundary conditions (including interface relations at $\tilde{x}_3 = \tilde{x}_m$) are specified. However, since we will not be concerned with the initial-value problem, but only the long-time solution corresponding to a (quasi-) steadily propagating deflagration, only the latter are required here. Thus, the required boundary conditions are given by

$$\alpha = \alpha_s \text{ for } \tilde{x} < \tilde{x}_m\,; \quad \tilde{u}_g \to 0\,, \quad \tilde{T} \to \tilde{T}_u\,, \quad \tilde{p}_g \to \tilde{p}_g^u \text{ as } \tilde{x} \to -\infty\,, \tag{9}$$

$$\tilde{p}_g = \tilde{p}_g^b \text{ for } \tilde{x} > \tilde{x}_m\,; \quad \alpha \to 1\,, \quad \tilde{u}_g \to \tilde{u}_g^b\,, \quad \tilde{T} \to \tilde{T}_b \text{ as } \tilde{x} \to +\infty\,, \tag{10}$$

where the burned temperature $\tilde{T}_b$, gas velocity $\tilde{u}_g^b$ and pressure $\tilde{p}_g^b$ are to be determined, except in the unconfined limit where, from Eq. (6b), $\tilde{p}_g^b = \tilde{p}_g^u$. The unburned and burned values $\tilde{\rho}_g^u$ and $\tilde{\rho}_g^b$ of the gas density then follow from the equation of state. We remark that the upstream boundary condition on the gas velocity is, except in the unconfined limit, merely a consistency condition in the present formulation, since it is implied by the corresponding upstream condition on pressure and the first of Eqs. (6a). Finally, denoting by $\pm$ superscripts quantities evaluated at $\tilde{x} = \tilde{x}_m^{\pm}$, the continuity and jump conditions across the melting surface are

$$\alpha^+ = \alpha^- = \alpha_s\,, \quad \tilde{u}_g^+ = \tilde{u}_g^-\,, \quad \tilde{u}_g^- = -\frac{\tilde{\kappa}(\alpha_s)}{\alpha_s \tilde{\mu}_g} \frac{\partial \tilde{p}_g}{\partial \tilde{x}_3}\bigg|_{\tilde{x}=\tilde{x}_m^-}\,, \quad \tilde{p}_g^- = \tilde{p}_g^+ = \tilde{p}_g^b\,, \quad \tilde{T}^+ = \tilde{T}^- = \tilde{T}_m\,, \tag{11}$$

the third of which implies $\tilde{\partial} p_g / \partial \tilde{x}_3 \to 0$ in the infinite-permeability/unconfined limit $\tilde{\kappa} \to \infty$. In addition, overall conservation of enthalpy flux across $\tilde{x} = \tilde{x}_m$ is expressed, using Eq. (8), as

$$\begin{aligned} \left[(1-\alpha_s)\tilde{\lambda}_l + \alpha_s \tilde{\lambda}_g\right] \hat{\mathbf{n}}_m \cdot \tilde{\nabla}\tilde{T}\bigg|_{\tilde{x}=\tilde{x}_m^+} - \left[(1-\alpha_s)\tilde{\lambda}_s + \alpha_s \tilde{\lambda}_g\right] \hat{\mathbf{n}}_m \cdot \tilde{\nabla}\tilde{T}\bigg|_{\tilde{x}=\tilde{x}_m^-} \\ = (1-\alpha_s)\tilde{\rho}_s\, G_m^{-1} \frac{\partial \tilde{x}_m}{\partial \tilde{t}} \left[\tilde{\gamma}_s + (\tilde{c}_s - \tilde{c}_l)\tilde{T}_m\right]\,, \end{aligned} \tag{12}$$

where the geometric factor G_m and the unit normal $\hat{\mathbf{n}}_m$ are given by

$$G_m = \left[1 + (\partial \tilde{x}_m/\partial \tilde{x}_1)^2 + (\partial \tilde{x}_m/\partial \tilde{x}_2)^2\right]\,, \quad \hat{\mathbf{n}}_m = G_m^{-1}(-\partial \tilde{x}_m/\partial \tilde{x}_1, -\partial \tilde{x}_m/\partial \tilde{x}_2, 1)\,, \tag{13}$$

respectively, and where $\tilde{\gamma}_s$ is the heat of melting of the solid at temperature $\tilde{T} = 0$ ($\tilde{\gamma}_s$ being negative when melting is endothermic).

III. Nondimensionalizations and Further Approximations

The formulation presented above is meant to be a reasonable representation of certain classes of materials, such as the nitramine propellant HMX, that satisfy the main assumptions introduced

thus far. Typical values associated with the physical properties of two widely studied nitramines, HMX and RDX, are quoted in various places.[5,16] The only additional primary approximation that will be introduced below is the assumption, already alluded to in the previous sections, of gas-phase quasi-steadiness.[17–19] This approximation is common in analyzing the stability of deflagrations in nonporous propellants (though it can be relaxed under certain conditions[20–22]), and, for multidimensional stability analyses, has generally been accompanied by a quasi-planar assumption as well.[23] This notion of gas-phase quasi-steadiness, which is discussed in more detail in Ref. 9, is thus extended to the two-phase-flow problems associated with porous materials, and is a particularly convenient approximation for the present study in that both confined and unconfined geometries can then be treated within the same framework. However, we emphasize that even though the velocity field can be approximated as one-dimensional (due to the dominance of the normal component) by restricting the analysis to weakly nonplanar deflagrations, terms representing transverse diffusion of heat remain. As a result, the present formulation retains certain multidimensional gas-phase effects, and thus does not explicitly invoke gas-phase quasi-planarity as a simplifying assumption.

In proceeding with a reasonable nondimensionalization for the present class of problems, it is convenient to introduce a characteristic velocity $\tilde{U}$ defined as the speed of propagation $\tilde{U} = -d\tilde{x}_m/d\tilde{t}$ associated with the special case of a quasi-steady planar deflagration (an explicit expression for $\tilde{U}$ is presented in Sections IV and V). Assuming constant values for heat capacities and thermal conductivities, we then introduce the nondimensional variables

$$x = \frac{\tilde{\rho}_s \tilde{c}_s \tilde{U}}{\tilde{\lambda}_s}\tilde{x}\,, \quad t = \frac{\tilde{\rho}_s \tilde{c}_s \tilde{U}^2}{\tilde{\lambda}_s}\tilde{t}\,, \quad T_{s,l,g} = \frac{\tilde{T}_{s,l,g}}{\tilde{T}_u}\,, \quad u_{l,g} = \frac{\tilde{u}_{l,g}}{\tilde{U}}\,, \quad \rho_g = \frac{\tilde{\rho}_g}{\tilde{\rho}_g^u}\,, \quad p_g = \frac{\tilde{p}_g}{\tilde{p}_g^u}\,, \tag{14a}$$

where $\tilde{\rho}_g^u = \tilde{p}_g^u \tilde{W}_g / \tilde{R}^\circ \tilde{T}_u$ denotes the gas density at the unburned temperature $\tilde{T}_u$ and pressure $\tilde{p}_g^u$. In addition, the nondimensional parameters

$$\begin{gathered} r = \frac{\tilde{\rho}_l}{\tilde{\rho}_s}\,, \quad \hat{r} = \frac{\tilde{\rho}_g^u}{\tilde{\rho}_s}\,, \quad l = \frac{\tilde{\lambda}_l}{\tilde{\lambda}_s}\,, \quad \hat{l} = \frac{\tilde{\lambda}_g}{\tilde{\lambda}_s}\,, \quad b = \frac{\tilde{c}_l}{\tilde{c}_s}\,, \quad \hat{b} = \frac{\tilde{c}_g}{\tilde{c}_s}\,, \quad \gamma_s = \frac{\tilde{\gamma}_s}{\tilde{c}_s \tilde{T}_u}\,, \quad Q = \frac{\tilde{Q}}{\tilde{c}_s \tilde{T}_u}\,, \\ \kappa = \frac{\tilde{\rho}_s \tilde{c}_s \tilde{p}_g^u \tilde{\kappa}}{\tilde{\lambda}_s \tilde{\mu}_g}\,, \quad \hat{\pi} = \frac{\tilde{p}_g^u}{\tilde{\rho}_s \tilde{c}_s \tilde{T}_u} = \hat{r}\hat{b}\chi\,, \quad \chi = \frac{\gamma - 1}{\gamma}\,, \quad N = \frac{\tilde{E}_l}{\tilde{R}^\circ \tilde{T}_b}\,, \quad \Lambda = \frac{\tilde{\lambda}_s \tilde{A}}{\tilde{\rho}_s \tilde{c}_s \tilde{U}^2} e^{-N} \end{gathered} \tag{14b}$$

are defined, where γ is the ratio of specific heats for the gas. It may be remarked that Λ is the appropriate burning-rate eigenvalue, the determination of which will provide the quasi-steady, planar propagation speed $\tilde{U}$.

Transforming to the moving coordinate $\xi = x_3 - x_m(x_1, x_2, t)$, whose origin is thus defined to be x_m, and introducing the above nondimensionalizations, Eqs. (1) – (12) become

$$\frac{\partial \rho_g}{\partial t} + \frac{\partial}{\partial \xi}\left[\rho_g\left(u_g - \frac{\partial x_m}{\partial t}\right)\right] = 0\,, \quad \xi < 0\,, \tag{15}$$

$$\frac{\partial}{\partial t}\left[\alpha(\hat{r}\rho_g - r)\right] + \frac{\partial}{\partial \xi}\left[r(1-\alpha)\left(u_l - \frac{\partial x_m}{\partial t}\right) + \hat{r}\alpha\rho_g\left(u_g - \frac{\partial x_m}{\partial t}\right)\right] = 0\,, \quad \xi > 0\,, \tag{16}$$

$$\frac{\partial \alpha}{\partial t} - \frac{\partial}{\partial \xi}\left[(1-\alpha)\left(u_l - \frac{\partial x_m}{\partial t}\right)\right] = \Lambda(1-\alpha)\exp\left[N\left(1-\frac{T_b}{T}\right)\right], \quad \xi > 0, \tag{17}$$

$$\begin{aligned}\frac{\partial}{\partial t}\left[(1-\alpha_s+\hat{r}\hat{b}\alpha_s\rho_g)T\right] + (1-\alpha_s)\left(-\frac{\partial x_m}{\partial t}\right)\frac{\partial T}{\partial \xi} + \hat{r}\hat{b}\alpha_s\frac{\partial}{\partial \xi}\left[\left(u_g - \frac{\partial x_m}{\partial t}\right)\rho_g T\right] \\ = \nabla_m \cdot \left[(1-\alpha_s+\hat{l}\alpha_s)\nabla_m T\right] + \hat{\pi}\alpha_s\left(\frac{\partial p_g}{\partial t} - \frac{\partial x_m}{\partial t}\frac{\partial p_g}{\partial \xi}\right), \quad \xi < 0,\end{aligned} \tag{18}$$

$$\begin{aligned}\frac{\partial}{\partial t}\left[r(1-\alpha)(Q+bT) + \hat{r}\hat{b}\alpha\rho_g T\right] + \frac{\partial}{\partial \xi}\left[r(1-\alpha)\left(u_l - \frac{\partial x_m}{\partial t}\right)(Q+bT) + \hat{r}\hat{b}\alpha\left(u_g - \frac{\partial x_m}{\partial t}\right)\rho_g T\right] \\ = \nabla_m \cdot \left\{\left[l(1-\alpha)+\hat{l}\alpha\right]\nabla_m T\right\}, \quad \xi > 0,\end{aligned} \tag{19}$$

$$\rho_g T_g = p_g, \tag{20}$$

$$u_l = -\frac{1}{r}(1-r)\frac{\partial x_m}{\partial t}, \tag{21}$$

subject to the boundary and melting-surface conditions

$$\alpha = \alpha_s, \quad u_g = -\frac{\kappa(\alpha_s)}{\alpha_s}\frac{\partial p_g}{\partial \xi} \text{ for } \xi < 0; \quad T \to 1, \quad p_g \to 1 \text{ as } \xi \to -\infty, \tag{22}$$

$$p_g = p_g^b \text{ for } \xi > 0; \quad \alpha \to 1, \quad u_g \to u_g^b, \quad T \to T_b \text{ as } \xi \to +\infty, \tag{23}$$

$$\alpha^+ = \alpha^- = \alpha_s, \quad u_g^+ = u_g^-, \quad u_g^- = -\frac{\kappa(\alpha_s)}{\alpha_s}\frac{\partial p_g}{\partial \xi}\bigg|_{\xi=0^-}, \quad p_g^- = p_g^+ = p_g^b, \quad T^+ = T^- = T_m, \tag{24}$$

$$\begin{aligned}\left[l(1-\alpha_s)+\hat{l}\alpha_s\right]\hat{\mathbf{n}}_m \cdot \nabla_m T\Big|_{\xi=0^+} - \left[1-\alpha_s+\hat{l}\alpha_s\right]\hat{\mathbf{n}}_m \cdot \nabla_m T\Big|_{\xi=0^-} \\ = (1-\alpha_s)G_m^{-1}\frac{\partial x_m}{\partial t}\left[\gamma_s + (1-b)T_m\right],\end{aligned} \tag{25}$$

where $\nabla_m = \left(\partial/\partial x_1 - \{\partial x_m/\partial x_1\}\partial/\partial\xi, \partial/\partial x_2 - \{\partial x_m/\partial x_2\}\partial/\partial\xi, \partial/\partial\xi\right)$ is the gradient in the moving coordinate system. The limit $p_g^b \to 1$ and the elimination of the third of Eqs. (24) may be taken in the case of an infinitely permeable material and/or unconfined geometry.

In the quasi-steady gas-phase limit discussed above, the gas phase is regarded as steady with respect to $\xi = 0$, and thus time derivatives of gas-phase quantities in the moving coordinate system (*viz.* $\partial p_g/\partial t$, $\partial(\alpha\rho_g)/\partial t$ and $\partial(\alpha\rho_g T)/\partial t$) may be set to zero, so that with the use of Eq. (21), Eqs. (15) – (19) become

$$\frac{\partial}{\partial \xi}\left[\rho_g\left(u_g - \frac{\partial x_m}{\partial t}\right)\right] = 0, \quad \xi < 0, \tag{26}$$

$$r\frac{\partial \alpha}{\partial t} + \frac{\partial}{\partial \xi}\left[(1-\alpha)\frac{\partial x_m}{\partial t} - \hat{r}\alpha\rho_g\left(u_g - \frac{\partial x_m}{\partial t}\right)\right] = 0, \quad \xi > 0, \tag{27}$$

$$r\frac{\partial \alpha}{\partial t} + \frac{\partial}{\partial \xi}\left[(1-\alpha)\frac{\partial x_m}{\partial t}\right] = r\Lambda(1-\alpha)\exp\left[N\left(1-\frac{T_b}{T}\right)\right], \quad \xi > 0, \tag{28}$$

$$(1-\alpha_s)\frac{\partial T}{\partial t} - (1-\alpha_s)\frac{\partial x_m}{\partial t}\frac{\partial T}{\partial \xi} + \hat{r}\hat{b}\alpha_s \frac{\partial}{\partial \xi}\left[\left(u_g - \frac{\partial x_m}{\partial t}\right)\rho_g T\right] = \nabla_m \cdot \left[(1-\alpha_s+\hat{l}\alpha_s)\nabla_m T\right] - \hat{\pi}\alpha_s \frac{\partial x_m}{\partial t}\frac{\partial p_g}{\partial \xi}, \quad \xi < 0, \tag{29}$$

$$r\frac{\partial}{\partial t}\left[(1-\alpha)(Q+bT)\right] + \frac{\partial}{\partial \xi}\left[-(1-\alpha)\frac{\partial x_m}{\partial t}(Q+bT) + \hat{r}\hat{b}\alpha\left(u_g - \frac{\partial x_m}{\partial t}\right)\rho_g T\right] = \nabla_m \cdot \left\{\left[l(1-\alpha)+\hat{l}\alpha\right]\nabla_m T\right\}, \quad \xi > 0, \tag{30}$$

Equations (20) – (24), along with the equation of state (20) and the boundary/interface conditions (22) – (25), constitute the final model that will be considered below.

IV. The Burning-Rate Eigenvalue for Steady, Planar Combustion

Time-independent solutions of the final formulation given in the previous section correspond to either steady (unconfined) or quasi-steady (confined) deflagrations. In either case, the nondimensional propagation speed $\partial x_m/\partial t = -1$ by definition, and the classical problem is to determine the dimensional burning rate $\tilde{U}$ by obtaining an expression for the burning-rate eigenvalue Λ. Thus, first considering the more general case of a confined geometry, a solution is sought for the steady eigenvalue problem

$$\frac{d}{d\xi}\left[\frac{p_g}{T}(u_g+1)\right] = 0, \quad \xi < 0, \tag{31}$$

$$\frac{d}{d\xi}\left[(1-\alpha) + \hat{r}\alpha\frac{p_g}{T}(u_g+1)\right] = 0, \quad \xi > 0, \tag{32}$$

$$\frac{d}{d\xi}(1-\alpha) = -r\Lambda(1-\alpha)\exp\left[N\left(1-\frac{T_b}{T}\right)\right], \quad \xi > 0, \tag{33}$$

$$(1-\alpha_s)\frac{dT}{d\xi} + \hat{r}\hat{b}\alpha_s\frac{d}{d\xi}\left[p_g(u_g+1)\right] = \frac{d}{d\xi}\left[(1-\alpha_s+\hat{l}\alpha_s)\frac{dT}{d\xi}\right] + \hat{r}\hat{b}\chi\alpha_s\frac{dp_g}{d\xi}, \quad \xi < 0, \tag{34}$$

$$\frac{d}{d\xi}\left[(1-\alpha)(Q+bT) + \hat{r}\hat{b}\alpha p_g(u_g+1)\right] = \frac{d}{d\xi}\left\{\left[l(1-\alpha)+\hat{l}\alpha\right]\frac{dT}{d\xi}\right\}, \quad \xi > 0, \tag{35}$$

subject to the boundary and melting-surface conditions (22) – (25) which, when specialized to one dimension, become

$$\alpha = \alpha_s, \quad u_g = -\frac{\kappa(\alpha_s)}{\alpha_s}\frac{dp_g}{d\xi} \text{ for } \xi < 0; \quad T \to 1, \quad p_g \to 1 \text{ as } \xi \to -\infty, \tag{36}$$

$$p_g = p_g^b \text{ for } \xi > 0; \quad \alpha \to 1, \quad u_g \to u_g^b, \quad T \to T_b \text{ as } \xi \to +\infty, \tag{37}$$

$$\alpha^+ = \alpha^- = \alpha_s, \quad u_g^+ = u_g^- = -\frac{\kappa(\alpha_s)}{\alpha_s}\frac{dp_g}{d\xi}\bigg|_{\xi=0^-}, \quad p_g^- = p_g^+ = p_g^b, \quad T^+ = T^- = T_m, \tag{38}$$

$$\left[l(1-\alpha_s)+\hat{l}\alpha_s\right]\frac{dT}{d\xi}\bigg|_{\xi=0^+} - \left[1-\alpha_s+\hat{l}\alpha_s\right]\frac{dT}{d\xi}\bigg|_{\xi=0^-} = (1-\alpha_s)\left[-\gamma_s + (b-1)T_m\right]. \tag{39}$$

Here, the alternate expression for the coefficient $\hat{\pi}$ indicated in Eqs. (14b) has been used in the last term of Eq. (29), and the equation of state (20) has been used to give a closed problem for α, p_g, u_g, T and the eigenvalue Λ.

IV.1. Preliminary Analysis

A partial solution in the region $\xi < 0$, where chemical activity is absent, as well as expressions for T_b, u_g^b and $u_g(0) = u_g|_{\xi=0}$, are obtained as follows. From Eqs. (31) and the boundary conditions (36), we have

$$p_g(u_g + 1) = T\,, \quad \xi < 0\,, \tag{40}$$

and hence

$$u_g\big|_{\xi=0} = \frac{T_m}{p_g^b} - 1\,. \tag{41}$$

We observe from Eq. (40) that since $T \geq 1$, the gas velocity $u_g > -1$ in the gas/solid region $\xi < 0$. That is, consistent with a quasi-steady mode of burning, the speed of gas permeation into the solid must be less than the propagation speed of the deflagration. Equation (32) and the surface conditions (38) and (41) then imply

$$p_g^b(u_g + 1) = \frac{\alpha + \alpha_s(\hat{r} - 1)}{\hat{r}\alpha} T\,, \quad \xi > 0\,, \tag{42}$$

which, upon evaluation at $\xi = \infty$, determines u_g^b in terms of T_b as

$$u_g^b = \frac{1 - \alpha_s + \hat{r}\alpha_s}{\hat{r}} \left(\frac{T_b}{p_g^b}\right) - 1\,. \tag{43}$$

Turning attention to the energy equations (34) and (35), we may readily perform a single integration and use the above relationships to obtain

$$(1 - \alpha_s + \hat{r}\hat{b}\alpha_s)(T - 1) = (1 - \alpha_s + \hat{l}\alpha_s)\frac{dT}{d\xi} + \hat{r}\hat{b}\chi\alpha_s(p_g - 1)\,, \quad \xi < 0\,, \tag{44}$$

$$\Big[b(1-\alpha) + \hat{b}(\alpha - \alpha_s + \hat{r}\alpha_s)\Big]\, T = \Big[l(1-\alpha) + \hat{l}\alpha\Big]\, \frac{dT}{d\xi} - (1-\alpha)Q + \hat{b}(1 - \alpha_s + \hat{r}\alpha_s)T_b\,, \quad \xi > 0\,. \tag{45}$$

Thus, subtracting Eq. (44) evaluated at $\xi = 0^-$ from Eq. (45) evaluated at $\xi = 0^+$ and using the jump condition (39), we obtain an expression for T_b given by

$$T_b = \frac{(1 - \alpha_s)(Q + 1 + \gamma_s) + \hat{r}\hat{b}\alpha_s\left[1 + \chi(p_g^b - 1)\right]}{\hat{b}(1 - \alpha_s + \hat{r}\alpha_s)}\,, \tag{46}$$

which, from Eq. (43), determines u_g^b as

$$u_g^b = \frac{1}{\hat{r}\hat{b}p_g^b}\left[(1 - \alpha_s)(Q + 1 + \gamma_s - \hat{r}\hat{b}) - \hat{r}\hat{b}(p_g^b - 1)(1 - \alpha_s\chi)\right]\,. \tag{47}$$

We note that in the limit $p_g^b \to 1$, Eqs. (46) and (47) collapse to the results for unconfined burning, where in place of Darcy's law in the solid/gas region, $p_g = 1$ throughout.

It is clear from these results that, since $0 < \chi = 1 - 1/\gamma < 1$, T_b increases linearly with the overpressure $p_g^b - 1$, as shown in Fig. 2. It is readily seen that for small overpressures T_b decreases with increasing values of the porosity α_s, whereas at higher overpressures, the opposite trend is observed. Indeed, denoting the burned temperature at zero porosity by $T_b^0 = (Q + 1 + \gamma_s)/\hat{b}$, which is independent of p_g^b, we obtain from Eq. (46) that for $\alpha_s > 0$, $T_b = T_b^0$ at the critical value of overpressure given by $p_g^b - 1 = (T_b^0 - 1)/\chi$. For overpressures greater than this critical value, the preheating effect due to gas permeation is sufficient to overcome that due to a decrease in the amount of solid material, resulting in an increase in burned temperature above T_b^0. Subsequently, it is clear from Fig. 2 that the magnitude of the difference $T_b - T_b^0$ at a given value of the overpressure is an increasing function of α_s. In connection with this result, we observe from Eq. (47) and Fig. 3 that the burned gas velocity u_g^b is a monotonically decreasing function of the overpressure. In fact, for sufficiently large overpressures that satisfy the condition

$$p_g^b - 1 > \frac{1 - \alpha_s}{1 - \alpha_s \chi} \left(\frac{Q + 1 + \gamma_s}{\hat{r}\hat{b}} - 1 \right) = \frac{(1 - \alpha_s)(T_b^0 - \hat{r})}{\hat{r}(1 - \alpha_s \chi)}, \tag{48}$$

which depends on α_s, we find that u_g^b is negative, implying a gas flow in the upstream direction throughout the multi-phase flame. This is clearly illustrated in Fig. 3, which shows the curves for u_g^b as a function of $p_g^b - 1$ crossing the horizontal axis at the above critical value of the overpressure. Also shown in Fig. 3 is the value of the gas velocity $u_g(\xi)$ at the solid/liquid interface $\xi = 0$, which is only positive for relatively small values of the overpressure. In particular, from Eq. (41), $u_g(0)$ crosses the horizontal axis at the critical value $p_g^b - 1 = T_m - 1$, beyond which gas flow is directed into the solid/gas region, resulting in the preheating effect due to gas permeation as described above. Further solution of the problem in the liquid/gas region, which is necessary for the determination of the burning-rate eigenvalue, is considered in the following section.

Before proceeding with an analysis of the liquid/gas reaction region, we observe that the problem in the solid/gas region can be reduced to a scalar problem for the gas pressure p_g. In particular, from Eq. (40) and the Darcy formula for u_g in Eq. (36), T and thus u_g are given in terms of p_g by

$$T = p_g \left(1 - \frac{\kappa}{\alpha_s} \frac{dp_g}{d\xi} \right), \quad u_g = \frac{T}{p_g} - 1, \quad \xi < 0. \tag{49}$$

Substituting these results into Eq. (44) thus yields a second-order equation for p_g in the region $\xi < 0$ given by

$$(1 - \alpha_s + \hat{r}\hat{b}\alpha_s) \left[p_g \left(1 - \frac{\kappa}{\alpha_s} \frac{dp_g}{d\xi} \right) - 1 \right] = (1 - \alpha_s + \hat{l}\alpha_s) \frac{d}{d\xi} \left[p_g \left(1 - \frac{\kappa}{\alpha_s} \frac{dp_g}{d\xi} \right) \right] + \hat{r}\hat{b}\chi\alpha_s(p_g - 1), \tag{50}$$

subject to the boundary conditions

$$p_g = p_g^b, \quad \frac{dp_g}{d\xi} = \frac{\alpha_s}{\kappa} \left(1 - \frac{T_m}{p_g^b} \right) \text{ at } \xi = 0; \quad p_g \to 1 \text{ as } \xi \to -\infty, \tag{51}$$

where the second condition follows from the Darcy formula and Eq. (41) for u_g evaluated at $\xi = 0$. We note that the last condition, aside from being consistent with the first of Eqs. (49), is already built into Eq. (50) by virtue of the fact that Eq. (50) is really a first integral of Eq. (34). Had the above expression for T been substituted directly into the latter, a third-order equation for p_g would have been obtained, permitting the specification of the three boundary conditions (51). The problem (50) – (51), the solution of which will determine T and u_g according to Eqs. (49), will be treated in the section following the determination of the burning-rate eigenvalue.

IV.2. The Burning-Rate Eigenvalue

In order to determine the burning-rate eigenvalue, we must complete our analysis of the liquid/gas region $\xi > 0$. In this regard, Eqs. (28) and (36) constitute two equations for T and α in this region, with u_g then determined by Eq. (33) and the eigenvalue Λ determined by the boundary conditions. In order to handle the Arrhenius nonlinearity, we exploit the largeness of the nondimensional activation energy N and analyze the problem in the asymptotic limit $N \gg 1$. Since $p_g = p_g^b$ throughout the liquid/gas region, the analysis of the confined and unconfined problems is essentially the same for $\xi > 0$.

In the limit $N \to \infty$, all chemical activity is concentrated in a very thin region where T is within $O(1/N)$ of T_b. Denoting the location of this thin zone by $\xi_r > 0$, we see that the semi-infinite liquid/gas region is comprised of a preheat zone ($0 < \xi < \xi_r$) where chemical activity is exponentially small, the thin reaction zone where the chemical reaction goes to completion, and a burned region $\xi > \xi_r$. Thus, we conclude from Eq. (33) that

$$\alpha = \begin{cases} \alpha_s, & \xi < \xi_r \\ 1, & \xi > \xi_r \,, \end{cases} \tag{52}$$

and from Eqs. (42) and (43),

$$u_g = \begin{cases} T/p_g^b - 1, & 0 < \xi < \xi_r \\ \hat{r}^{-1}(1 - \alpha_s + \hat{r}\alpha_s)T_b/p_g^b - 1 = u_g^b, & \xi > \xi_r \,, \end{cases} \tag{53}$$

Since T is within $O(1/N)$ of T_b in the reaction zone, the analysis of this thin region requires the use of a stretched coordinate (see below). As a result, T is continuous with respect to the $O(1)$ outer variable ξ at $\xi = \xi_r$, and thus the gas velocity jumps across $\xi = \xi_r$ by the amount

$$u_g\big|_{\xi=\xi_r^+} - u_g\big|_{\xi=\xi_r^-} = \frac{1}{\hat{r}}(1 - \hat{r})(1 - \alpha_s)\frac{T_b}{p_g^b} \,, \tag{54}$$

which is positive assuming the unburned gas density is less than that of the solid (i.e., $\hat{r} < 1$). Finally, using Eq. (52), Eq. (45) may be integrated a second time to completely determine the outer temperature profile in the liquid/gas region as

$$T(\xi) = \begin{cases} B + (T_m - B)\exp\left[\dfrac{b(1-\alpha_s) + \hat{r}\hat{b}\alpha_s}{l(1-\alpha_s) + \hat{l}\alpha_s}\xi\right], & 0 < \xi < \xi_r \\ T_b \,, & \xi > \xi_r \,, \end{cases} \tag{55}$$

where

$$B \equiv \frac{(1-\alpha_s)(1+\gamma_s) + \hat{r}\hat{b}\alpha_s\left[1+\chi(p_g^b-1)\right]}{b(1-\alpha_s)+\hat{r}\hat{b}\alpha_s}\,. \tag{56}$$

We note that $T(\xi)$ for $\xi < 0$ is still to be determined from Eq. (49) and the solution of the pressure problem (50) – (51), as described in the next section; however, it is not required for the determination of the burning-rate eigenvalue Λ. The location ξ_r of the reaction zone, which appears as a sheet on the scale of the outer variable ξ, is thus determined by Eqs. (55) from continuity of T as

$$\xi_r = \frac{l(1-\alpha_s)+\hat{l}\alpha_s}{b(1-\alpha_s)+\hat{r}\hat{b}\alpha_s}\ln\left(\frac{T_b-B}{T_m-B}\right)\,. \tag{57}$$

The determination of the burning-rate eigenvalue Λ, as well as the spatial evolution of the variables α and u_g (which are discontinuous on the scale of the outer variable ξ), requires an analysis of the thin reaction-zone region in the vicinity of ξ_r. We thus introduce a stretched inner variable η and a normalized temperature variable Θ defined by

$$\Theta = \frac{T-1}{T_b-1}\,, \qquad \eta = \beta(\xi-\xi_r)\,, \qquad \beta \equiv (1-T_b^{-1})N \gg 1\,, \tag{58}$$

where β is the Zel'dovich number, and seek solutions in the form of the expansions

$$\begin{aligned} &\alpha \sim \alpha_0 + \beta^{-1}\alpha_1 + \beta^{-2}\alpha_2 + \cdots\,, \quad && u_g \sim u_0 + \beta^{-1}u_1 + \beta^{-2}u_2 + \cdots\,, \\ &\Theta \sim 1 + \beta^{-1}\theta_1 + \beta^{-2}\theta_2 + \cdots\,, && \Lambda \sim \beta(\Lambda_0 + \beta^{-1}\Lambda_1 + \beta^{-2}\Lambda_2 + \cdots)\,. \end{aligned} \tag{59}$$

The coefficients in the expansion of u_g are readily determined from Eq. (42) in terms of the α_i and θ_i, which themselves are obtained from solving the sequence of inner problems that arise from substituting the above expansions into Eqs. (33) and (45) and matching with the outer solutions for $\xi < \xi_r$ and $\xi > \xi_r$. In particular, at leading order the inner problem is given by

$$\frac{d\alpha_0}{d\eta} = r\Lambda_0(1-\alpha_0)\,e^{\theta_1}\,, \tag{60}$$

$$\left[l + (\hat{l}-l)\alpha_0\right]\frac{d\theta_1}{d\eta} = \frac{D}{T_b-1}(1-\alpha_0)\,, \tag{61}$$

subject to the matching conditions

$$\alpha_0 \to \alpha_s\,, \quad \theta_1 \sim E\eta \ \text{ as } \ \eta \to -\infty\,, \tag{62}$$

$$\alpha_0 \to 1\,, \quad \theta_1 \to 0 \ \text{ as } \ \eta \to +\infty\,. \tag{63}$$

Here, D and E are defined as

$$D \equiv (b-\hat{b})T_b + Q\,, \qquad E \equiv \frac{1}{T_b-1}\frac{dT}{d\xi}\bigg|_{\xi=\xi_r^-}\,, \tag{64}$$

where the latter is calculated from Eq. (55).

The problem (60) - (63) is now readily solved by employing α_0 as the independent variable. Thus, using Eq. (60), Eq. (61) may be written as

$$r\Lambda_0 \left[l + (\hat{l} - l)\alpha_0 \right] e^{\theta_1} \frac{d\theta_1}{d\alpha_0} = \frac{D}{T_b - 1}, \tag{65}$$

which is readily integrated from α_s (at $\eta = -\infty$) to any $\alpha_0 \leq 1$ to give

$$e^{\theta_1(\alpha_0)} = \frac{D}{(T_b - 1) r \Lambda_0} \int_{\alpha_s}^{\alpha_0} \frac{d\alpha_0}{l + (\hat{l} - l)\alpha_0}. \tag{66}$$

Evaluating the latter at $\alpha_0 = 1$ (at which $\theta_1 = 0$) thus determines the leading-order coefficient Λ_0 in the expansion of the burning-rate eigenvalue as

$$\Lambda_0 = \begin{cases} \dfrac{D}{(T_b - 1) r (\hat{l} - l)} \ln \left[\dfrac{\hat{l}}{l + (\hat{l} - l)\alpha_s} \right], & l \neq \hat{l} \\ \dfrac{D}{(T_b - 1) r l} (1 - \alpha_s), & l = \hat{l}, \end{cases} \tag{67}$$

and using this result in Eq. (66) for arbitrary α_0 then determines $\theta_1(\alpha_0)$ as

$$\theta_1(\alpha_0) = \begin{cases} \ln \left(\dfrac{\ln \left[l + (\hat{l} - l)\alpha_0 \right] - \ln \left[l + (\hat{l} - l)\alpha_s \right]}{\ln \hat{l} - \ln \left[l + (\hat{l} - l)\alpha_s \right]} \right), & \hat{l} \neq l \\ \ln \left(\dfrac{\alpha_0 - \alpha_s}{1 - \alpha_s} \right), & \hat{l} = l. \end{cases} \tag{68}$$

The determination of $\alpha_0(\eta)$, and hence $\theta_1(\eta)$, then follows directly from Eq. (60).

From Eq. (67) and the definition of Λ according to the last of Eqs. (14b) and (59), the leading-order expression for the dimensional propagation speed $\tilde{U}$ is given by

$$\tilde{U}^2 \sim \frac{r(T_b - 1)\tilde{A}(p_g^b)}{\beta D \tilde{\rho}_s \tilde{c}_s} e^{-N} \cdot \tilde{f}(\tilde{\lambda}_g, \tilde{\lambda}_l) = \frac{r T_b^2}{(b - \hat{b})T_b + Q} \cdot \frac{\tilde{A}(p_g^b)}{\tilde{\rho}_s \tilde{c}_s N_u} e^{-N_u/T_b} \cdot \tilde{f}(\tilde{\lambda}_g, \tilde{\lambda}_l), \tag{69}$$

where $N_u = \tilde{E}_l / \tilde{R}^\circ \tilde{T}_u = N T_b$ is independent of T_b and the last factor, which contains the complete dependence of the burning rate on the thermal conductivities, is given by

$$\tilde{f}(\tilde{\lambda}_g, \tilde{\lambda}_l) = \begin{cases} \dfrac{\tilde{\lambda}_g - \tilde{\lambda}_l}{\ln \left(\tilde{\lambda}_g / [\tilde{\lambda}_l + (\tilde{\lambda}_g - \tilde{\lambda}_l)\alpha_s] \right)}, & \tilde{\lambda}_g \neq \tilde{\lambda}_l \\ \tilde{\lambda}_l / (1 - \alpha_s), & \tilde{\lambda}_g = \tilde{\lambda}_l. \end{cases} \tag{70}$$

The expression (69) for the burning rate, though virtually identical in form for both the confined problem and the unconfined problem obtained in the limit of constant pressure ($p_g^b = 1$), nonetheless differs implicitly for the two types of problems through the linear dependence of T_b on the overpressure $p_g^b - 1$. In particular, because there is an exponential dependence of the reaction

rate on T_b, relatively small changes in T_b can produce significant modifications in the propagation speed.

In order to analyze explicitly the dependence of the burning rate on the overpressure, it is convenient to define the normalized burning rate $U^* = \tilde{U}(p_g^b)/\tilde{U}(1)$, where the argument denotes the value of p_g^b. Consequently, from Eq. (69), we obtain $U^* = U_n[\tilde{A}(p_g^b)/\tilde{A}(1)]^{1/2}$, where the coefficient U_n is given by

$$U_n = \frac{T_b(p_g^b)}{T_b(1)} \left[\frac{(b-\hat{b})T_b(1)+Q}{(b-\hat{b})T_b(p_g^b)+Q} \right]^{1/2} \exp\left[\frac{N_u}{2} \left(\frac{1}{T_b(1)} - \frac{1}{T_b(p_g^b)} \right) \right], \tag{71}$$

and where T_b as a function of p_g^b is given by Eq.(46). In this form, it is readily seen, since T_b is a linearly increasing function of overpressure and the nondimensional activation-energy parameter N_u is typically very large (its definition, given below Eq. (69), is in terms of the *unburned* temperature $\tilde{T}_u$), that U_n is exponentially sensitive to T_b and hence p_g^b. Thus, as the overpressure $p_g^b - 1$ increases from zero, the burning rate increases exponentially (Fig. 4), reflecting the sensitivity to the corresponding increase in the rate of gas permeation into the solid/gas region given by Eq. (41). We remark that this result cannot be predicted with a constant-pressure model appropriate for unconfined deflagrations, since in that case, the gas flow is always in the downstream direction (if one imposes the upstream boundary condition that u_g vanish) and an increase in pressure then serves only to decrease T_b due to the increase in the gas density ($\hat{r}$ increases) that absorbs more of the heat of reaction. In the present context, the upstream gas density $\hat{r}$ remains constant, and an increase in overpressure serves to preheat the unburned solid through enhanced permeation of the burned gas into the solid/gas region. In the limit of large overpressures, T_b^{-1} becomes small and the exponential factor in Eq. (71) approaches a constant value. Consequently, in the range of large overpressures, the dependence of U_n on p_g^b becomes algebraic. This is also illustrated in Fig. 4, in which case (since $b = \hat{b}$) the saturated dependence of U_n on p_g^b is linear. We note that this feature (exponential transition to an algebraic pressure-dependent burning rate) is qualitatively consistent with most experiments in Crawford-type (large volume) bombs that indicate a rapid increase in the burning rate frequently associated with the onset of convective burning,[6,24,25] followed by a less dramatic pressure dependence that is typically represented in the form Ap^n.

V. Analysis of the Gas-Permeation Layer

The pressure-driven permeation of hot gases into the unburned porous solid has been shown to be a critical factor in causing the rapid increase in the burning rate associated with the onset of convective burning. However, this implies nontrivial pressure and velocity profiles in this region in order to satisfy the ambient upstream boundary conditions on these variables. Thus, although the calculation of the burning-rate eigenvalue in the previous section did not require a detailed knowledge of the actual solution profiles in the solid/gas region, it being sufficient to determine the results (40) – (41) for u_g, there is nonetheless a strong interest in computing these profiles in

order to better understand the role of convection in these types of two-phase-flow problems. Since gas permeation is clearly a strong function of the pressure difference across the deflagration, it is convenient to define an overpressure variable $p = p_g - 1$, in terms of which the pressure problem (50) – (51) can be written as

$$(1-\alpha_s+\hat{r}\hat{b}\alpha_s)\left[p-\frac{\kappa}{\alpha_s}(p+1)\frac{dp}{d\xi}\right]=(1-\alpha_s+\hat{l}\alpha_s)\frac{d}{d\xi}\left[p-\frac{\kappa}{\alpha_s}(p+1)\frac{dp}{d\xi}\right]+\hat{r}\hat{b}\chi\alpha_s p\,, \tag{72}$$

subject to

$$p=p_b=p_g^b-1\,,\quad \frac{dp}{d\xi}=\frac{\alpha_s}{\kappa}\left(1-\frac{T_m}{p_b+1}\right)\ \text{ at }\ \xi=0\,;\quad p\to 0\ \text{ as }\ \xi\to-\infty\,. \tag{73}$$

Since our goal is a qualitative understanding of gas-permeation effects, it suffices to obtain approximate solutions using asymptotic methods. In particular, we may introduce a bookkeeping parameter $\epsilon \ll 1$ and consider the realistic parameter regime in which $\hat{r}$, $\hat{l}$, α_s, and κ/α_s are all $O(\epsilon)$, where we note that the permeability κ is usually proportional to some power of α_s that is greater than unity.[13,26] That is, we scale these small quantities as

$$\alpha_s=\alpha_s^*\epsilon\,,\quad \kappa=\kappa^*\epsilon^2\,,\quad \hat{r}=\hat{r}^*\epsilon\,,\quad \hat{l}=\hat{l}^*\epsilon\,, \tag{74}$$

in terms of which Eqs. ((72) and (73) become

$$(1-\epsilon\alpha_s^*+\epsilon^2\hat{r}^*\hat{b}\alpha_s^*)\left[p-\epsilon\frac{\kappa^*}{\alpha_s^*}(p+1)\frac{dp}{d\xi}\right]=(1-\epsilon\alpha_s^*+\epsilon^2\hat{l}^*\alpha_s^*)\frac{d}{d\xi}\left[p-\epsilon\frac{\kappa^*}{\alpha_s^*}(p+1)\frac{dp}{d\xi}\right]+\epsilon^2\hat{r}^*\hat{b}\chi\alpha_s^* p\,, \tag{75}$$

$$p=p_b=p_g^b-1\,,\quad \frac{dp}{d\xi}=\epsilon^{-1}\frac{\alpha_s^*}{\kappa^*}\left(1-\frac{T_m}{p_b+1}\right)\ \text{ at }\ \xi=0\,;\quad p\to 0\ \text{ as }\ \xi\to-\infty\,. \tag{76}$$

The problem given by Eqs. (75) and (76) has been analyzed[12] for two primary cases of interest; namely $p \sim O(1)$ and $p \sim O(\epsilon^{-1})$, corresponding to two different magnitudes of p_g^b. The results of this analysis are as follows. For $O(1)$ overpressures, the second condition in Eq. (76) suggests that there is an $O(\epsilon)$ boundary layer in the vicinity of $\xi = 0$. Consequently, a stretched coordinate $\eta = \xi/\epsilon$ is introduced to describe the solution within the boundary layer, which is then matched to the outer solution for negative $O(1)$ values of ξ. In this fashion, the leading-order composite solution is determined as

$$p=\sim p_0(\xi/\epsilon)+(T_m-1)(e^{\xi}-1)\,, \tag{77}$$

where the leading-order inner solution p_0, which has been functionally expressed in terms of the outer variable ξ, is given implicitly by

$$\frac{\alpha_s^*}{\kappa^*}(\xi/\epsilon)=p_0-p_b+T_m\ln\left(\frac{p_0-T_m+1}{p_b-T_m+1}\right)\,. \tag{78}$$

The boundary-layer (inner), outer and composite solutions are illustrated in Fig. 5. From Eq. (77), the gas velocity in the solid/gas region is, in turn, given by

$$u_g=-\frac{\kappa}{\alpha_s}\frac{dp}{d\xi}\sim -1+\frac{T_m}{p_0(\xi/\epsilon)+1}-\epsilon\frac{\kappa^*}{\alpha^*}(T_m-1)\,e^{\xi}\,. \tag{79}$$

We observe that $p_0(\xi/\epsilon) \to T_m - 1$ as ξ approaches O(1) negative values, and thus, as indicated in Fig. 5, it is clear that gas permeation for O(1) overpressures is only significant in the thin boundary layer adjacent to the solid/liquid interface, assuming $p_b > T_m - 1$. Although this last qualification is by far the typical case (since $T_m - 1 = \tilde{T}_m/\tilde{T}_u - 1$ is not likely to be larger than unity), it is nonetheless of interest to point out that the structure of the solution will change as p_b approaches the value $T_m - 1$ due to the fact that the gradient of pressure at $\xi = 0$, which has been scaled as $O(\epsilon^{-1})$ in Eq. (76), will cease to be large in that limit. Indeed, for small overpressures ($0 < p_b < T_m - 1$), the pressure gradient becomes negative at $\xi = 0$, indicating, according to Eqs. (36) and (41), a gas flow out of the solid in the downstream direction, as in the case of an unconfined deflagration.

The other primary case of interest in many applications is the limit in which the overpressure itself becomes large. In that case, it is useful to rescale p in Eqs. (75) and (76) by defining the scaled overpressure $P = \epsilon p$. In terms of P, Eqs. (75) and (76) become

$$(1-\epsilon\alpha_s^*+\epsilon^2\hat{r}^*\hat{b}\alpha_s^*)\left[P - \frac{\kappa^*}{\alpha_s^*}(P+\epsilon)\frac{dP}{d\xi}\right] = (1-\epsilon\alpha_s^*+\epsilon^2\hat{l}^*\alpha_s^*)\frac{d}{d\xi}\left[P - \frac{\kappa^*}{\alpha_s^*}(P+\epsilon)\frac{dP}{d\xi}\right] + \epsilon^2\hat{r}^*\hat{b}\chi\alpha_s^* P\,, \tag{80}$$

$$P = P_b \equiv \frac{1}{\epsilon}(p_g^b - 1)\,, \quad \frac{dP}{d\xi} = \frac{\alpha_s^*}{\kappa^*}\left(1 - \frac{\epsilon T_m}{P_b+\epsilon}\right) \text{ at } \xi = 0\,; \quad P \to 0 \text{ as } \xi \to -\infty\,. \tag{81}$$

There is now no reason to suspect a boundary layer near $\xi = 0$, but a straightforward perturbation solution on the ξ - scale leads to the approximate solution

$$P \sim P_0 = \begin{cases} (\alpha_s^*/\kappa^*)(\xi+\xi_0)\,, & -\xi_0 < \xi \le 0 \\ 0\,, & \xi < -\xi_0 \end{cases}\,, \quad \xi_0 = \frac{\kappa^*}{\alpha_s^*}P_b\,, \tag{82}$$

which is valid everywhere except at $\xi = -\xi_0$ where the derivative is discontinuous. This kink in the solution thus suggests the existence of a thin corner layer in that vicinity. Hence, we interpret Eq. (82) as the leading-order outer solution, and proceed to construct an inner solution in a thin region centered about $\xi = -\xi_0$. In particular, it turns out that the proper scales on which to analyze this layer are $P \sim O(\epsilon)$ and $\xi \sim O(\epsilon)$. The result of a matching of the solution in this region with the outer solution (82) is the uniform composite approximation[12]

$$\frac{\alpha_s^*}{\kappa^*}(\xi+\xi_0) \sim P + \epsilon \ln\left(\frac{P}{P_b}\right)\,. \tag{83}$$

The outer and composite solutions (82) and (83) for the scaled overpressure P are illustrated in Fig. 6. It is clear that in this case, gas permeation extends an O(1) distance into the gas/solid region, although, as in the previous case of O(1) overpressures, the extent of gas permeation remains, because of the relative smallness of the permeability κ, an order of magnitude less than that of the overpressure itself.

VI. An Asymptotic Model for Nonsteady, Nonplanar Burning

The solution analyzed above constitutes the special case of a quasi-steady, planar deflagration, and is not necessarily the only long-time solution of the final model presented in Section III. For example, one generally expects that there exist parameter thresholds beyond which such a solution loses stability to one or more nonsteady and/or nonplanar modes of burning. In order to perform such stability analyses, it is appropriate to extend the previous one-dimensional large activation-energy analysis of the reaction zone to obtain a more tractable flame-sheet type of model. In such a model, the reaction zone is asymptotically relegated to an infinitesimally thin region, and the (outer) solutions on either side of this reaction front are connected by derived jump and continuity conditions. This effectively simplifies the problem by allowing consideration of a coupled problem for the reactionless outer variables, and is the basis on which most modern analytical stability analyses are based.

VI.1. The Outer Problem

In the limit of large activation energy, the reaction zone collapses to a reaction front located at $x_3 = x_r(x_1, x_2, t) > x_m(x_1, x_2, t)$, and it is convenient to shift the (nonorthogonal) moving coordinate by defining the new coordinate $\zeta = \xi - (x_r - x_m)$, or in terms of the original variables, $\zeta = x_3 - x_r(x_1, x_2, t)$. In this new coordinate system, the origin is thus defined to be at $x_3 = x_r$, and in terms of ζ, the problem defined by Eqs. (15) - (25) becomes, given the assumption of a quasi-steady gas phase with respect to the new coordinate system and the expression (21) for u_l,

$$\frac{\partial}{\partial\zeta}\left[\rho_g\left(u_g - \frac{\partial x_r}{\partial t}\right)\right] = 0\,, \quad \zeta < -(x_r - x_m)\,, \tag{84}$$

$$r\frac{\partial\alpha}{\partial t} + \frac{\partial}{\partial\zeta}\left[(1-\alpha)\left(\frac{\partial x_m}{\partial t} + r\left\{\frac{\partial x_r}{\partial t} - \frac{\partial x_m)}{\partial t}\right\}\right) - \hat{r}\alpha\rho_g\left(u_g - \frac{\partial x_r}{\partial t}\right)\right] = 0\,, \quad \zeta > -(x_r - x_m)\,, \tag{85}$$

$$r\frac{\partial\alpha}{\partial t} + \frac{\partial}{\partial\zeta}\left[(1-\alpha)\left(\frac{\partial x_m}{\partial t} + r\left\{\frac{\partial x_r}{\partial t} - \frac{\partial x_m}{\partial t}\right\}\right)\right] = r\Lambda(1-\alpha)\exp\left[N\left(1 - \frac{T_b}{T}\right)\right]\,, \quad \zeta > -(x_r - x_m), \tag{86}$$

$$\begin{aligned}(1-\alpha_s)\frac{\partial T}{\partial t} + \frac{\partial}{\partial\zeta}\left\{\left[(1-\alpha_s)\left(-\frac{\partial x_r}{\partial t}\right) + \hat{r}\hat{b}\alpha_s\left(u_g - \frac{\partial x_r}{\partial t}\right)\rho_g\right]T\right\} \\ = \nabla_r\cdot\left\{\left[1 - \alpha_s + \hat{l}\alpha_s\right]\nabla_r T\right\} - \hat{\pi}\alpha_s\frac{\partial x_r}{\partial t}\frac{\partial p_g}{\partial\zeta}\,, \quad \zeta < -(x_r - x_m)\,,\end{aligned} \tag{87}$$

$$\begin{aligned}r\frac{\partial}{\partial t}\left[(1-\alpha)(Q+bT)\right] + \frac{\partial}{\partial\zeta}\left[(1-\alpha)\left(-\frac{\partial x_m}{\partial t} - r\left\{\frac{\partial x_r}{\partial t} - \frac{\partial x_m}{\partial t}\right\}\right)(Q+bT)\right] \\ + \frac{\partial}{\partial\zeta}\left[\hat{r}\hat{b}\alpha\left(u_g - \frac{\partial x_r}{\partial t}\right)\rho_g T\right] = \nabla_r\cdot\left\{\left[l(1-\alpha) + \hat{l}\alpha\right]\nabla_r T\right\}\,, \quad \zeta > -(x_r - x_m)\,,\end{aligned} \tag{88}$$

subject to the equation of state (20) and the conditions

$$\alpha = \alpha_s\,, \quad u_g = -\frac{\kappa(\alpha_s)}{\alpha_s}\frac{\partial p_g}{\partial\zeta} \text{ for } \zeta \le -(x_r - x_m)\,; \quad p_g \to 1 \ (u_g \to 0)\,, \quad T \to 1 \text{ as } \zeta \to -\infty\,, \tag{89}$$

$$p_g = p_g^b \text{ for } \zeta > -(x_r - x_m); \quad \alpha \to 1, \quad T \to T_b \text{ as } \zeta \to +\infty, \tag{90}$$

$$T\big|_{\zeta=-(x_r-x_m)} = T_m, \tag{91}$$

$$\left[l(1-\alpha_s) + \hat{l}\alpha_s\right] \hat{\mathbf{n}}_m \cdot \nabla_r T\Big|_{\zeta=-(x_r-x_m)^+} - \left(1 - \alpha_s + \hat{l}\alpha_s\right) \hat{\mathbf{n}}_m \cdot \nabla_r T\Big|_{\zeta=-(x_r-x_m)^-} = G_m^{-1} \frac{\partial x_m}{\partial t}(1-\alpha_s)\left[\gamma_s + (1-b)T_m\right], \tag{92}$$

where all variables are implicitly continuous across the melting surface $\zeta = -(x_r - x_m)$ and, analogous to the definition of ∇_m given below Eq. (25), the operator $\nabla_r = \left(\partial/\partial x_1 - \{\partial x_r/\partial x_1\}\partial/\partial\zeta, \partial/\partial x_2 - \{\partial x_r/\partial x_2\}\partial/\partial\zeta, \partial/\partial\zeta\right)$ is the nondimensional gradient operator expressed in terms of the moving coordinate system attached to the reacting surface. The final burned temperature T_b that appears in the boundary condition (90) for the general nonsteady, nonplanar problem is the same as that calculated for the special case of steady, planar burning analyzed in Section IV, and is thus given by Eq. (46).

As in the special case of steady, planar combustion, we again consider the limit of large activation energy ($N \gg 1$), in which case all chemical activity and heat release associated with the reaction term in Eq. (86) are confined to a thin $O(N^{-1})$ reaction zone at $\zeta = 0$. In this way, the original distributed-reaction problem is reduced to a pair of reactionless problems in the outer regions $\zeta < 0$ and $\zeta > 0$, the solutions of which must be matched to the reaction-zone solution valid in the thin inner region $|\zeta| \ll 1$. The result is an asymptotic model for the outer variables, subject to nonlinear jump conditions across $\zeta = 0$ that depend on local conditions there, and an evolution equation for $x_r(x_1, x_2, t)$. With this asymptotic simplification, the outer solution of Eqs. (84) – (86) for the gas-phase volume fraction and velocity is given by

$$\alpha = \begin{cases} \alpha_s, & \zeta < 0 \\ 1, & \zeta > 0, \end{cases} \tag{93}$$

$$u_g = \begin{cases} -(T/p_g - 1)\partial x_r/\partial t, & \zeta < -(x_r - x_m) \\ -(T/p_g^b - 1)\partial x_r/\partial t, & -(x_r - x_m) < \zeta < 0 \\ (T/p_g^b)\, g(x_1, x_2, t) + \partial x_r/\partial t, & \zeta > 0, \end{cases} \tag{94}$$

where the first of these indicates that all variation in the volume-fraction variable α is confined to the inner reaction zone analyzed in the next subsection and the second expresses u_g in terms of the local temperature and the instantaneous propagation speed of the reaction zone, with the "constant" of integration $g(x_1, x_2, t) = (p_g^b/T_b)(u_g|_{\zeta\to+\infty} - \partial x_r/\partial t)$ to be determined. The top expression in Eq. (94) may be combined with the expression for u_g in Eq. (89) (Darcy's law) to give the additional relation

$$T = p_g \left[1 + \frac{\kappa}{\alpha_s}\frac{\partial p_g}{\partial \zeta}\left(\frac{\partial x_r}{\partial t}\right)^{-1}\right], \quad \zeta < -(x_r - x_m), \tag{95}$$

which is the appropriate generalization of Eq. (49). By use of these results and the equation of state (20) in Eqs. (87) and (88), the outer problem becomes

$$(1-\alpha_s)\frac{\partial T}{\partial t} + (1 - \alpha_s + \hat{r}\hat{b}\alpha_s)\left(-\frac{\partial x_r}{\partial t}\right)\frac{\partial T}{\partial \zeta} = (1 - \alpha_s + \hat{l}\alpha_s)\nabla_r^2 T - \hat{\pi}\alpha_s \frac{\partial x_r}{\partial t}\frac{\partial p_g}{\partial \zeta}, \quad \zeta < -(x_r - x_m), \tag{96}$$

$$rb(1-\alpha_s)\frac{\partial T}{\partial t}+\left[rb(1-\alpha_s)+\hat{r}\hat{b}\alpha_s\right]\left(-\frac{\partial x_r}{\partial t}\right)\frac{\partial T}{\partial \zeta}-b(1-r)(1-\alpha_s)\frac{\partial x_m}{\partial t}\frac{\partial T}{\partial \zeta}$$
$$=\left[l(1-\alpha_s)+\hat{l}\alpha_s\right]\nabla_r^2 T\,,\quad -(x_r-x_m)<\zeta<0\,, \tag{97}$$

$$\hat{r}\hat{b}g\frac{\partial T}{\partial \zeta}=\hat{l}\nabla_r^2 T\,,\quad \zeta>0\,, \tag{98}$$

subject to the boundary and interface conditions (89) – (92) on T and p_g. From the expression below Eq. (92) for ∇_r, the Laplacian operator ∇_r^2 in the (x_1,x_2,ζ) coordinate system is given by

$$\nabla_r^2=\frac{\partial^2}{\partial x_1^2}+\frac{\partial^2}{\partial x_2^2}+G_r^2\frac{\partial^2}{\partial \zeta^2}-2\frac{\partial x_r}{\partial x_1}\frac{\partial^2}{\partial x_1\partial\zeta}-2\frac{\partial x_r}{\partial x_2}\frac{\partial^2}{\partial x_2\partial\zeta}-\left(\frac{\partial^2 x_r}{\partial x_1^2}+\frac{\partial^2 x_r}{\partial x_2^2}\right)\frac{\partial}{\partial\zeta}\,, \tag{99}$$

where $G_r^2=1+(\partial x_r/\partial x_1)^2+(\partial x_r/\partial x_2)^2$. We observe that substitution of the relation (95) into Eq. (96) gives a nonlinear partial differential equation for p_g, analogous to the ordinary result (50) for steady, planar burning. These conditions, however, are still not sufficient to completely determine the solution for the outer variables. To do so requires additional jump and continuity conditions across the thin reaction zone located at $\zeta=0$, as well as an expression for the gas-velocity function $g(x_1,x_2,t)$ in the region $\zeta>0$, which necessitates an analysis of the inner reaction-zone problem.

The derivation of two of the additional conditions needed to close the outer problem may be obtained directly from an integration of Eq. (88) across the thin reaction region; *i.e.*, from $\zeta=0^-$ to $\zeta=0^+$. Using the results (93) and (94), and accounting for the fact that quantities such as α, T, $\alpha u_g T$, αT, $(1-\alpha)T$, $\alpha\partial T/\partial\zeta$ and $(1-\alpha)\partial T/\partial\zeta$ behave, in the limit of large activation energy, as distributions there, the continuity and jump relations

$$T\big|_{\zeta=0^-}=T\big|_{\zeta=0^+} \tag{100}$$

and

$$\left\{\hat{r}\hat{b}g+\left[(1-\alpha_s)rb+\alpha_s\hat{r}\hat{b}\right]\frac{\partial x_r}{\partial t}+(1-\alpha_s)(1-r)b\frac{\partial x_m}{\partial t}\right\}T\big|_{\zeta=0}$$
$$+(1-\alpha_s)Q\left[r\frac{\partial x_r}{\partial t}+(1-r)\frac{\partial x_m}{\partial t}\right]-(l-\hat{l})(1-\alpha_s)\left(\frac{\partial x_r}{\partial x_1}\frac{\partial T}{\partial x_1}+\frac{\partial x_r}{\partial x_2}\frac{\partial T}{\partial x_2}\right)\Big|_{\zeta=0} \tag{101}$$
$$=G_r^2\left\{\hat{l}\frac{\partial T}{\partial\zeta}\Big|_{\zeta=0^+}-\left[l(1-\alpha_s)+\hat{l}\alpha_s\right]\frac{\partial T}{\partial\zeta}\Big|_{\zeta=0^-}\right\}$$

are obtained. The structure of the inner reaction zone, with suitable matching of solutions in that region to the outer solutions, must now be addressed to obtain an additional jump condition across $\zeta=0$ and an expression for the function g introduced in Eq. (94). We thus employ the method of matched asymptotic expansions and seek solutions to the coupled outer problems in the form of the expansions $T\sim T^{(0)}+N^{-1}T^{(1)}+N^{-2}T^{(2)}+\cdots$, and similarly for the gas-velocity function g. Hence, to leading order, the outer equations obtained thus far are given by Eqs. (89) - (101) with T and g replaced by $T^{(0)}$ and $g^{(0)}$, respectively.

VI.2. The Reaction-Zone Solutions

Spatial variations in the reaction-zone solutions in the normal (ζ) direction occur on a short, of order N^{-1}, length scale relative to that of the outer solutions. Accordingly, it is appropriate to introduce the stretched normal coordinate η defined by

$$\eta = \beta\zeta = \beta(x_3 - x_r)\,, \tag{102}$$

where β is the Zel'dovich number defined in the last of Eqs. (58), and it is also convenient to introduce again the normalized temperature variable $\Theta = (T-1)/(T_b-1)$. Solutions to the inner problem are then sought in the form of the expansions

$$\begin{aligned}
\alpha &\sim \alpha_0 + \beta^{-1}\alpha_1 + \beta^{-2}\alpha_2 + \cdots\,,\\
u_g &\sim u_0 + \beta^{-1}u_1 + \beta^{-2}u_2 + \cdots\,,\\
\Theta &\sim 1 + \beta^{-1}\theta_1 + \beta^{-2}\theta_2 + \cdots\,,\\
\Lambda &\sim \beta(\Lambda_0 + \beta^{-1}\Lambda_1 + \beta^{-2}\Lambda_2 + \cdots)\,,
\end{aligned} \tag{103}$$

where the latter represents the appropriate expansion of the burning-rate eigenvalue of the basic solution corresponding to steady, planar burning. We note that since $p_g = p_g^b$ throughout the gas/liquid region, no such expansion is required for p_g and thus, provided the assumption of gas-phase quasi-steadiness remains valid, the development in this section is valid for both unconfined and confined geometries. Substituting these expansions and definitions into Eqs. (85), (86) and (88) and equating coefficients of like powers of β, the leading-order inner problem is derived in the following fashion. Beginning with Eq. (85), we obtain

$$\left(r - \hat{r}\frac{p_g^b}{T_b}\right)\frac{\partial x_r}{\partial t}\frac{\partial \alpha_0}{\partial \eta} + (1-r)\frac{\partial x_m}{\partial t}\frac{\partial \alpha_0}{\partial \eta} + \hat{r}\frac{p_g^b}{T_b}\frac{\partial}{\partial \eta}(\alpha_0 u_0) = 0\,. \tag{104}$$

Integrating this result and applying the matching conditions $\alpha_0 \to \alpha_s$ and $u_0 \to -(T_b/p_g^b - 1)\partial x_r/\partial t$ as $\eta \to -\infty$, we obtain an expression for u_0 as

$$u_0 = \frac{T_b(\alpha_0 - \alpha_s)}{p_g^b \hat{r}\alpha_0}\left[(\hat{r}-r)\frac{\partial x_r}{\partial t} - (1-r)\frac{\partial x_m}{\partial t}\right] - \left(\frac{T_b}{p_g^b} - 1\right)\frac{\partial x_r}{\partial t}\,. \tag{105}$$

From the matching conditions $\alpha_0 \to 1$ and $u_0 \to (T_b/p_g^b)g^{(0)} + \partial x_r/\partial t$ as $\eta \to +\infty$, an expression for the outer gas-velocity function $g^{(0)}(x_1, x_2, t)$ in the region $\zeta > 0$ is then found to be

$$g^{(0)}(x_1, x_2, t) = \frac{1-\alpha_s}{\hat{r}}\left[(\hat{r}-r)\frac{\partial x_r}{\partial t} - (1-r)\frac{\partial x_m}{\partial t}\right] - \frac{\partial x_r}{\partial t}\,, \tag{106}$$

which is needed in Eq. (98).

Utilizing Eq. (105) for the gas velocity, we find that the remaining part of the leading-order inner problem for α_0 and θ_1 is now determined from Eqs. (86) and (88) as

$$\left[r\frac{\partial x_r}{\partial t} + (1-r)\frac{\partial x_m}{\partial t}\right]\frac{\partial \alpha_0}{\partial \eta} = -r\Lambda_0(1-\alpha_0)\,e^{\theta_1}\,, \tag{107}$$

$$\left[r\frac{\partial x_r}{\partial t}+(1-r)\frac{\partial x_m}{\partial t}\right]\left[Q+(b-\hat{b})T_b\right]\frac{\partial \alpha_0}{\partial \eta}=(T_b-1)G_r^2\frac{\partial}{\partial \eta}\left\{\left[l+(\hat{l}-l)\alpha_0\right]\frac{\partial \theta_1}{\partial \eta}\right\}, \tag{108}$$

subject to the matching conditions

$$\alpha_0 \to 1\,, \quad \theta_1 \sim \Theta^{(1)}\big|_{\zeta=0+} \text{ as } \eta \to +\infty \tag{109}$$

and

$$\alpha_0 \to \alpha_s\,, \quad \theta_1 \sim \Theta^{(1)}\big|_{\zeta=0-} + \eta\frac{\partial \Theta^{(0)}}{\partial \zeta}\Big|_{\zeta=0-} \text{ as } \eta \to -\infty\,, \tag{110}$$

where, consistent with the definition of Θ, the $\Theta^{(i)}$ are defined as $\Theta^{(i)}=(T^{(i)}-1)/(T_b-1)$. We note that since spatial variations in the normal (ζ) direction are large relative to those in the transverse direction and those with respect to time, as reflected in the transformation (102), the reaction-zone problem (107) - (110) is always quasi-steady and quasi-planar, independent of the assumption of quasi-steadiness for the outer gas-phase equations introduced earlier. Thus, integrating Eq. (108) using Eq. (109), and then transforming to α_0 as the independent coordinate according to Eq. (107), we obtain a first-order equation for θ_1 given by

$$r\Lambda_0 e^{\theta_1}\frac{\partial \theta_1}{\partial \alpha_0}=H_{m,r}^2\frac{Q+(b-\hat{b})T_b}{T_b-1}\cdot\frac{1}{l+(\hat{l}-l)\alpha_0}\,, \tag{111}$$

where

$$H_{m,r}=-G_r^{-1}\left[r\frac{\partial x_r}{\partial t}+(1-r)\frac{\partial x_m}{\partial t}\right]. \tag{112}$$

Equation (111) may then be integrated with respect to α_0 by using Eq. (110) to give

$$r\Lambda_0 e^{\theta_1}=H_{m,r}^2\frac{Q+(b-\hat{b})T_b}{T_b-1}\cdot\begin{cases}(\hat{l}-l)^{-1}\left\{\ln\left[l+(\hat{l}-l)\alpha_0\right]-\ln\left[l+(\hat{l}-l)\alpha_s\right]\right\}, & \hat{l}\neq l\\ l^{-1}\left(\alpha_0-\alpha_s\right), & \hat{l}=l\,.\end{cases} \tag{113}$$

For the special case of steady, planar burning, $\partial x_m/\partial t=\partial x_r/\partial t=-1$, and $\Theta^{(1)}|_{\zeta=0+}=0$ in the matching condition (109). Since Eq. (113) must hold for all solutions, these conditions imply the result (67) for the leading-order coefficient Λ_0 in the last of the expansions (103) for the burning-rate eigenvalue. Here, T_b was given in Eq. (46), a result that in fact applies to the more general nonsteady, nonplanar problem given the assumption of a quasi-steady gas phase and the specification of p_g^b.

For the general nonsteady, nonplanar problem, Eqs. (67), (113) and the matching condition (109) yield the local temperature-dependent propagation law

$$H_{m,r}=\exp\left(\frac{1}{2}\Theta^1\big|_{\zeta=0+}\right). \tag{114}$$

Equation (114) introduces the next-order outer variable Θ^1 into the analysis, but this additional complication, which is fundamental to this type of analysis,[22] can be circumvented in an approximate fashion by truncating the inner expansion for Θ given in Eq. (103) after the $O(\beta^{-1})$ term,

so that the matching condition (109) implies that $\Theta^{(1)}\big|_{\zeta=0} = \beta(\Theta\big|_{\zeta=0} - 1)$. Reverting back to the original outer temperature variable T, we find that Eq. (114) may be expressed as

$$-r\frac{\partial x_r}{\partial t} - (1-r)\frac{\partial x_m}{\partial t} = \left[1 + \left(\frac{\partial x_r}{\partial x_1}\right)^2 + \left(\frac{\partial x_r}{\partial x_2}\right)^2\right]^{1/2} \exp\left(-\frac{\beta}{2}\cdot\frac{T_b - T\big|_{\zeta=0}}{T_b - 1}\right), \tag{115}$$

where we have used the definition (112) for $H_{m,r}$. Substitution of Eq. (115) and the expression (106) for g into Eq. (101) then leads to the result

$$\begin{aligned}\hat{l}\frac{\partial T}{\partial \zeta}\bigg|_{\zeta=0^+} - \left[l + (\hat{l}-l)\alpha_s\right]\frac{\partial T}{\partial \zeta}\bigg|_{\zeta=0^-} + (1-\alpha_s)(l-\hat{l})G_r^{-2}\left(\frac{\partial x_r}{\partial x_1}\frac{\partial T}{\partial x_1} + \frac{\partial x_r}{\partial x_2}\frac{\partial T}{\partial x_2}\right)\bigg|_{\zeta=0} \\ = -(1-\alpha_s)\left[Q + (b-\hat{b})T\big|_{\zeta=0}\right] G_r^{-1}\exp\left(-\frac{\beta}{2}\cdot\frac{T_b - T\big|_{\zeta=0}}{T_b - 1}\right),\end{aligned} \tag{116}$$

which, if we retain Eq. (115), replaces Eq. (101) as the required jump condition across the thin reaction zone. When the outer solution is approximated (truncated) by setting $T \approx T^{(0)}$ and $g \approx g^{(0)}$, the derived conditions (100) and (101), the propagation law (115), and the expression (106) for the outer gas-velocity function g close the outer problem (89) – (92), (93) - (98).

VI.3. Summary of the Asymptotic Model

The model derived in the previous two subsections constitutes an asymptotic formulation, valid for large activation energies, of deflagration in porous energetic materials for the case of a thermally expansive, quasi-steady gas phase. In this regime, the reaction zone becomes thin relative to the convective-diffusive structure of the deflagration wave, in such a way that both the jump condition across the reaction sheet and the propagation law that governs its motion display a sensitivity to local temperature perturbations. This sensitivity is of a finite, but exponential, form that is induced by the original Arrhenius nature of the reaction rate in the asymptotic limit described above. It is helpful to collect the above results for future reference. Hence, the asymptotic model, expressed in nonorthogonal coordinates (x_1, x_2, ζ) attached to the reaction surface ($\zeta = 0$), is given by

$$\begin{aligned}(1-\alpha_s)\begin{Bmatrix}1\\ rb\\ 0\end{Bmatrix}\frac{\partial T}{\partial t} - \begin{Bmatrix}1+\alpha_s(\hat{r}\hat{b}-1)\\ rb+\alpha_s(\hat{r}\hat{b}-rb)\\ \hat{r}\hat{b}\end{Bmatrix}\frac{\partial x_r}{\partial t}\frac{\partial T}{\partial \zeta} \\ - (1-\alpha_s)\left[(1-r)\begin{Bmatrix}0\\ b\\ \hat{b}\end{Bmatrix}\frac{\partial x_m}{\partial t} + (r-\hat{r})\begin{Bmatrix}0\\ 0\\ \hat{b}\end{Bmatrix}\frac{\partial x_r}{\partial t}\right]\frac{\partial T}{\partial \zeta} \\ = \begin{Bmatrix}1+\alpha_s(\hat{l}-1)\\ l+\alpha_s(\hat{l}-l)\\ \hat{l}\end{Bmatrix}\nabla_r^2 T - \hat{\pi}\alpha_s\begin{Bmatrix}1\\ 0\\ 0\end{Bmatrix}\frac{\partial x_r}{\partial t}\frac{\partial p_g}{\partial \zeta}, \quad \begin{matrix}\zeta < -(x_r - x_m)\\ -(x_r - x_m) < \zeta < 0\\ \zeta > 0,\end{matrix}\end{aligned} \tag{117}$$

$$T = p_g\left[1 + \frac{\kappa}{\alpha_s}\frac{\partial p_g}{\partial \zeta}\left(\frac{\partial x_r}{\partial t}\right)^{-1}\right], \quad \zeta < -(x_r - x_m), \tag{118}$$

$$-r\frac{\partial x_r}{\partial t} - (1-r)\frac{\partial x_m}{\partial t} = G_r \exp\left(-\frac{\beta}{2}\cdot\frac{T_b - T\big|_{\zeta=0}}{T_b - 1}\right), \tag{119}$$

subject to

$$T \to p_g \to 1 \text{ as } \zeta \to -\infty, \quad T \to T_b \text{ as } \zeta \to +\infty, \tag{120}$$

$$T = T_m \text{ at } \zeta = -(x_r - x_m), \quad p_g = p_g^b \text{ for } \zeta \geq -(x_r - x_m), \tag{121}$$

$$\left(-\frac{\partial x_m}{\partial x_1}, -\frac{\partial x_m}{\partial x_2}, 1\right)\cdot\left\{\left[l + \alpha_s(\hat{l} - l)\right]\nabla_r T\big|_{\zeta=-(x_r-x_m)^+} - \left[1 + \alpha_s(\hat{l} - 1)\right]\nabla_r T\big|_{\zeta=-(x_r-x_m)^-}\right\}$$
$$= \frac{\partial x_m}{\partial t}(1-\alpha_s)\left[\gamma_s + (1-b)T_m\right], \tag{122}$$

$$T\big|_{\zeta=0^-} = T\big|_{\zeta=0^+}, \tag{123}$$

$$\hat{l}\frac{\partial T}{\partial \zeta}\bigg|_{\zeta=0^+} - \left[l + (\hat{l} - l)\alpha_s\right]\frac{\partial T}{\partial \zeta}\bigg|_{\zeta=0^-} + (1-\alpha_s)(l-\hat{l})G_r^{-2}\left(\frac{\partial x_r}{\partial x_1}\frac{\partial T}{\partial x_1} + \frac{\partial x_r}{\partial x_2}\frac{\partial T}{\partial x_2}\right)\bigg|_{\zeta=0}$$
$$= -(1-\alpha_s)\left[Q + (b-\hat{b})T\big|_{\zeta=0}\right]G_r^{-1}\exp\left(-\frac{\beta}{2}\cdot\frac{T_b - T\big|_{\zeta=0}}{T_b - 1}\right), \tag{124}$$

where the dot in Eq. (122) represents the scalar product of the vector on the left with the operator ∇_r given below Eq. (92), and where expressions for $\nabla_r^2 = \nabla_r \cdot \nabla_r$ and G_r were given in and below Eq. (99). Equations (117) – (124) constitute a closed boundary-value problem for x_r, x_m, T and p_g, an equation for the latter being obtained from the combination of Eqs. (117) and (118) in the region $\zeta < -(x_r - x_m)$, and may be solved subject to arbitrary initial conditions. In many applications, however, one is primarily concerned with the long-time basic solution corresponding to a steady, planar deflagration, as described by the formulation derived in the previous section, and its stability. We also note that the porosity α has been reduced to a simple step function by the asymptotic formulation and that other quantities of interest, such as the gas velocity (94), are given in terms of x_r, x_m, p_g and T according to the formulas derived previously.

VII. A Basic Solution and its Linear Stability

As an illustration of the usefulness of the asymptotic model derived above, we consider the stability of a steady, planar deflagration in the unconfined limit $p_g^b = 1$, which implies that $p_g = 1$ throughout. A basic solution of the model (117) - (124) in that case, corresponding to a steadily propagating planar deflagration and denoted by a zero superscript, is given by the solution constructed in Section IV, namely

$$x_m^0 = -t, \quad x_r^0 = x_m^0 + \frac{l(1-\alpha_s) + \hat{l}\alpha_s}{b(1-\alpha_s) + \hat{r}\hat{b}\alpha_s}\ln\left(\frac{T_b - B}{T_m - B}\right), \tag{125}$$

$$T^0(\zeta) = \begin{cases} 1 + (T_m - 1)\exp\left[\dfrac{1+\alpha_s(\hat{r}\hat{b}-1)}{1+\alpha_s(\hat{l}-1)}\left(\zeta + x_r^0 - x_m^0\right)\right], & \zeta < -(x_r^0 - x_m^0) \\ B + (T_m - B)\exp\left[\dfrac{b(1-\alpha_s)+\hat{r}\hat{b}\alpha_s}{l(1-\alpha_s)+\hat{l}\alpha_s}\left(\zeta + x_r^0 - x_m^0\right)\right], & -(x_r^0 - x_m^0) < \zeta < 0 \\ T_b = \dfrac{(1-\alpha_s)(Q+1+\gamma_s)+\hat{r}\hat{b}\alpha_s}{\hat{b}\left[1+\alpha_s(\hat{r}-1)\right]}, & \zeta > 0\,, \end{cases} \tag{126}$$

where

$$B \equiv \frac{(1-\alpha_s)(1+\gamma_s)+\hat{r}\hat{b}\alpha_s}{b(1-\alpha_s)+\hat{r}\hat{b}\alpha_s}\,, \tag{127}$$

and, from Eqs. (94) and (106), the steady, planar gas-phase velocity u_g^0 is given by

$$u_g^0 = \begin{cases} T - 1, & \zeta < 0 \\ \hat{r}^{-1}\left[(1-\hat{r})(1-\alpha_s) + (T_b - 1)(1 - \alpha_s + \alpha_s\hat{r})\right], & \zeta > 0\,. \end{cases} \tag{128}$$

The burning-rate eigenvalue and propagation speed were given by Eqs. (67), (69) and (70), but are not needed explicitly in the stability analysis that follows. Here, we are particularly interested in the effects of the porosity α_s, in the realistic limit of small gas-to-solid density ratio $\hat{r}$, on the stability of steady, planar deflagration given by the basic solution (125) – (128). As shown below, the value of the burned temperature plays a critical role in determining the corresponding neutral stability boundary, in part because the propagation velocity is exponentially sensitive to T_b in the large activation-energy regime. From the last line of Eq. (128), T_b has the behavior

$$T_b = \frac{1}{\hat{b}}\left[Q + 1 + \gamma_s - \hat{r}\frac{\alpha_s}{1-\alpha_s}\left(Q + 1 + \gamma_s - \hat{b}\right) + \mathrm{O}(\hat{r}^2)\right] \tag{129}$$

for $\hat{r} \ll 1$. Since the nondimensional heat release Q is typically significantly larger than unity, whereas the specific heat capacity ratio $\hat{b}$ is generally not significantly larger than unity, the final burned temperature, and hence the steady mass burning rate, decrease with increasing porosity and increasing gas density in the unconfined limit. However, as discussed in Section IV (Fig. 3), the opposite trend is predicted for the confined problem once the overpressure achieves a critical value.

Using the derived asymptotic model, the linear stability analysis of the basic solution (125) - (128) follows a standard approach[9]. Briefly, perturbation variables $\phi_m(x_1, x_2, t)$, $\phi_r(x_1, x_2, t)$ and $\tau(x_1, x_2, \zeta, t)$ are defined according to

$$x_m = x_m^0 + \phi_m\,, \quad x_r = x_r^0 + \phi_r\,, \quad T = T^0(\zeta) + \tau + \phi_r\frac{dT^0}{d\zeta}\,. \tag{130}$$

These definitions are substituted into the asymptotic model defined by Eqs. (117) - (124), and the equations are linearized with respect to the perturbation variables to obtain a linear problem for ϕ_m, ϕ_r and τ given by

$$\begin{aligned} (1-\alpha_s)\frac{\partial\tau}{\partial t} + \left[1+\alpha_s(\hat{r}\hat{b}-1)\right]\frac{\partial\tau}{\partial\zeta} - \hat{r}\hat{b}\alpha_s\frac{\partial\phi_r}{\partial t}\frac{dT^0}{d\zeta} \\ = \left[1+\alpha_s(\hat{l}-1)\right]\left(\frac{\partial^2\tau}{\partial x_1^2} + \frac{\partial^2\tau}{\partial x_2^2} + \frac{\partial^2\tau}{\partial\zeta^2}\right), \quad \zeta < -(x_r^0 - x_m^0)\,, \end{aligned} \tag{131}$$

$$rb(1-\alpha_s)\frac{\partial\tau}{\partial t}+\left[b+\alpha_s(\hat{r}\hat{b}-b)\right]\frac{\partial\tau}{\partial\zeta}-\left[\hat{r}\hat{b}\alpha_s\frac{\partial\phi_r}{\partial t}+b(1-r)(1-\alpha_s)\frac{\partial\phi_m}{\partial t}\right]\frac{dT^0}{d\zeta}$$
$$=\left[l+\alpha_s(\hat{l}-l)\right]\left(\frac{\partial^2\tau}{\partial x_1^2}+\frac{\partial^2\tau}{\partial x_2^2}+\frac{\partial^2\tau}{\partial\zeta^2}\right),\quad -(x_r^0-x_m^0)<\zeta<0\,, \tag{132}$$

$$\hat{b}\left[1+\alpha_s(\hat{r}-1)\right]\frac{\partial\tau}{\partial\zeta}=\hat{l}\left(\frac{\partial^2\tau}{\partial x_1^2}+\frac{\partial^2\tau}{\partial x_2^2}+\frac{\partial^2\tau}{\partial\zeta^2}\right),\quad \zeta>0\,, \tag{133}$$

$$-r\frac{\partial\phi_r}{\partial t}-(1-r)\frac{\partial\phi_m}{\partial t}=\frac{\beta}{2(T_b-1)}\tau\big|_{\zeta=0^+}\,, \tag{134}$$

subject to

$$\tau\to 0\ \text{ as }\ \zeta\to\pm\infty\,, \tag{135}$$

$$\left(\tau+\phi_m\frac{dT^0}{d\zeta}\right)\Big|_{\zeta=-(x_r^0-x_m^0)^-}=\left(\tau+\phi_m\frac{dT^0}{d\zeta}\right)\Big|_{\zeta=-(x_r^0-x_m^0)^+}=0\,, \tag{136}$$

$$\left[l+\alpha_s(\hat{l}-l)\right]\left(\frac{\partial\tau}{\partial\zeta}+\phi_m\frac{d^2T^0}{d\zeta^2}\right)\Big|_{\zeta=-(x_r^0-x_m^0)^+}-\left[1+\alpha_s(\hat{l}-1)\right]\left(\frac{\partial\tau}{\partial\zeta}+\phi_m\frac{d^2T^0}{d\zeta^2}\right)\Big|_{\zeta=-(x_r^0-x_m^0)^-}$$
$$=-\frac{\partial\phi_m}{\partial t}(1-\alpha_s)\left[-\gamma_s+(b-1)T_m\right], \tag{137}$$

$$\tau\big|_{\zeta=0^+}=\left(\tau+\phi_r\frac{dT^0}{d\zeta}\right)\Big|_{\zeta=0^-}\,, \tag{138}$$

$$\hat{l}\frac{\partial\tau}{\partial\zeta}\Big|_{\zeta=0^+}-\left[l+\alpha_s(\hat{l}-l)\right]\left(\frac{\partial\tau}{\partial\zeta}+\phi_r\frac{d^2T^0}{d\zeta^2}\right)\Big|_{\zeta=0^-}$$
$$=-\frac{1}{2}(1-\alpha_s)\left[\frac{\beta Q}{T_b-1}+(b-\hat{b})\left(2+\frac{\beta T_b}{T_b-1}\right)\right]\tau\big|_{\zeta=0^+}\,, \tag{139}$$

where we have used the fact that $dT^0/d\zeta=0$ for $\zeta>0$.

From Eqs. (130), steady, planar burning clearly corresponds to the trivial solution $\phi_m=\phi_r=\tau=0$, whereas nontrivial solutions to the linear stability problem are sought in the form

$$\left\{\begin{array}{c}\phi_m\\ \phi_r\\ \tau\end{array}\right\}=e^{i(\omega t\pm k_1x_1\pm k_2x_2)}\left\{\begin{array}{c}c_m\\ 1\\ \sigma(\zeta)\end{array}\right\}, \tag{140}$$

which has been normalized by setting the coefficient of ϕ_r equal to unity. Equations (131) - (133) and Eq. (135) then determine the function $\sigma(\zeta)$ as

$$\sigma(\zeta)=\left\{\begin{array}{ll}c_1e^{p\zeta}+i\omega(i\omega\hat{b}_1+k^2)^{-1}b_0b_1(T_m-1)e^{b_1(\zeta+x_r^0-x_m^0)}, & \zeta<-(x_r^0-x_m^0)\\ c_2e^{q-\zeta}+c_3e^{q+\zeta}+i\omega(i\omega\hat{b}_3+k^2)^{-1}(\hat{b}_0-b_4c_m)b_2(T_b-B)e^{b_2\zeta}, & -(x_r^0-x_m^0)<\zeta<0\\ c_4e^{\hat{s}\zeta}, & \zeta>0\,,\end{array}\right. \tag{141}$$

where the c_i are constants of integration, and the other quantities that appear in Eq. (141) are given by

$$b_0 = \frac{\hat{r}\hat{b}\alpha_s}{1+\alpha_s(\hat{l}-1)}, \quad \hat{b}_0 = \frac{\hat{r}\hat{b}\alpha_s}{l+\alpha_s(\hat{l}-l)}, \quad b_1 = \frac{1+\alpha_s(\hat{r}\hat{b}-1)}{1+\alpha_s(\hat{l}-1)}, \quad \hat{b}_1 = \frac{1-\alpha_s}{1+\alpha_s(\hat{l}-1)},$$
$$b_2 = \frac{b+\alpha_s(\hat{r}\hat{b}-b)}{l+\alpha_s(\hat{l}-l)}, \quad \hat{b}_3 = \frac{rb(1-\alpha_s)}{l+\alpha_s(\hat{l}-l)}, \quad b_4 = \frac{b(r-1)(1-\alpha_s)}{l+\alpha_s(\hat{l}-l)}, \quad b_5 = \frac{\hat{b}}{\hat{l}}\left[1+\alpha_s(\hat{r}-1)\right], \tag{142}$$

and

$$p = \frac{1}{2}\left[b_1 + \sqrt{b_1^2 + 4(i\omega\hat{b}_1 + k^2)}\right], \quad q_\pm = \frac{1}{2}\left[b_2 \pm \sqrt{b_2^2 + 4(i\omega\hat{b}_3 + k^2)}\right],$$
$$\hat{s} = \frac{1}{2}\left[b_5 - \sqrt{b_5^2 + 4k^2}\right]. \tag{143}$$

The remaining conditions embodied in Eqs. (134) and Eqs. (136) – (139) serve to determine the c_i and the dispersion relation $\omega(k)$, where $k = \sqrt{k_1^2 + k_2^2}$.

VIII. Analysis of the Dispersion Relation

The linear stability analysis is completed here for a representative case in which $r = b = l = 1$, corresponding to the neglect of differences between the physical properties of the solid and liquid phases of the material. While this restriction is introduced in order to reduce algebraic complexity, it clearly can be relaxed if there is interest in other values of these parameters. As a result, $b_2 = b_1$, $\hat{b}_0 = b_0$, $\hat{b}_3 = \hat{b}_1$ (which implies that $q_+ = p$) and $b_4 = 0$. Then, from Eqs. (133) and Eqs. (136) - (138), the coefficients in Eq. (141) are determined as

$$c_1 = -(T_m - 1)b_1 e^{q_+(x_r^0 - x_m^0)}\left[c_m + \frac{i\omega b_0}{i\omega\hat{b}_1 + k^2}\right], \quad c_4 = -2i\omega\frac{T_b - 1}{\beta},$$
$$c_2 = (B-1)b_1\frac{e^{q_-(x_r^0 - x_m^0)}}{q_- - q_+}\left[c_m(q_- + i\omega) + \frac{i\omega b_0 q_-}{i\omega\hat{b}_1 + k^2}\right],$$
$$c_3 = -b_1\frac{e^{q_+(x_r^0 - x_m^0)}}{q_- - q_+}\Big\{c_m\left[(B-1)(q_+ + i\omega) + (T_m - 1)(q_- - q_+)\right] + \frac{i\omega b_0}{i\omega\hat{b}_1 + k^2}\left[(T_m - 1)(q_- - q_+) + q_+(B-1)\right]\Big\} \tag{144}$$

where $x_r^0 - x_m^0$ was given by the second of Eqs. (125) and

$$c_m = \frac{1}{\mathcal{D}}\left[(T_b - 1)\left(b_1 + \frac{2i\omega}{\beta}\right) - (B-1)b_1 + (T_b - B)\frac{i\omega b_0 b_1}{i\omega\hat{b}_1 + k^2}\right]e^{-q_+(x_r^0 - x_m^0)}$$
$$+ \frac{i\omega b_0 b_1}{\mathcal{D}(i\omega\hat{b}_1 + k^2)}\left[q_-(B-1)\frac{e^{(q_- - q_+)(x_r^0 - x_m^0)} - 1}{q_- - q_+} - (T_m - B)\right], \tag{145}$$
$$\mathcal{D} = b_1(T_m - 1) - (B-1)b_1(q_- - q_+)^{-1}\left[(q_- + i\omega)e^{(q_- - q_+)(x_r^0 - x_m^0)} - (q_+ + i\omega)\right].$$

We remark that, in light of the above simplification, all effects due to melting of the solid are embodied in the parameter γ_s. In the limit that the heat of melting becomes negligible ($\gamma_s \to 0$), we have $B \to 1$ and hence $c_2 \to 0$. In that case, the functional form of the temperature function $\sigma(\zeta)$ is the same on either side of $\zeta = -(x_r^0 - x_m^0)$, and the melting surface becomes effectively "invisible".

An equation for the dispersion relation $\omega(k)$ is now obtained by substituting the results given thus far into Eq. (139). The result is, in terms of the coefficients defined above,

$$\hat{l}\hat{s}c_4 - (1-\alpha_s+\hat{l}\alpha_s)\left[q_-c_2 + q_+c_3 + b_1^2(T_b - B)\right] = -(1-\alpha_s)\left[\beta\frac{Q+(1-\hat{b})T_b}{2(T_b-1)} + 1 - \hat{b}\right]c_4, \quad (146)$$

where s and $q_\pm$ depend on $i\omega$ and k according to their definitions given above. This is a fairly complicated dispersion relation, but typically, the gas density is small compared with that of the condensed phases, the thermal conductivity of the gas is correspondingly small, and the heat of melting is small compared with the thermal enthalpy. For these reasons, the gas-to-solid/liquid density ratio $\hat{r}$ is treated as a small parameter, and the scalings

$$\hat{l} = \hat{l}^*\hat{r}\,, \quad \gamma_s = \gamma_s^*\hat{r}\,. \quad (147)$$

are introduced for the corresponding conductivity ratio $\hat{l}$ and the nondimensional heat of melting γ_s, where the scaled values $\hat{l}^*$ and γ_s^* are considered to be of order unity. The dispersion relation $\omega(k)$ is then expanded as

$$\omega \sim \omega_0 + \omega_1\hat{r} + \omega_2\hat{r}^2 + \cdots\,. \quad (148)$$

Associated expansions of all quantities in Eq. (146) that depend on these small parameters are then performed, keeping the overall heat release Q_0 with respect to the solid, $Q_0 = Q + \gamma_s$, a fixed parameter. Under this constraint, there is an expansion of the burned temperature T_b given by

$$T_b \sim T_b^0 + \hat{r}T_b^1 + \cdots\,, \quad T_b^0 = \frac{Q_0+1}{\hat{b}}\,, \quad T_b^1 = -\frac{\alpha_s}{1-\alpha_s}(T_b^0 - 1)\,. \quad (149)$$

In addition, the expansions

$$B - 1 \sim \gamma_s^*\hat{r}\,, \quad \hat{l}\hat{s} \sim \mathrm{O}(\hat{r}^2)\,, \quad b_1 \sim 1 + \frac{\alpha_s}{1-\alpha_s}(\hat{b} - \hat{l}^*)\hat{r} + \cdots\,, \quad \hat{b}_1 \sim 1 - \frac{\alpha_s}{1-\alpha_s}\hat{l}^*\hat{r} + \cdots\,, \quad (150)$$

and

$$\begin{aligned} q_\pm &\sim q_\pm^0 + q_\pm^1\hat{r} + \cdots\,, \quad q_\pm^0 = \frac{1}{2}\left[1 \pm \sqrt{1 + 4(i\omega_0 + k^2)}\right], \\ q_\pm^1 &= \frac{1}{2}\cdot\frac{\alpha_s}{1-\alpha_s}\left[\hat{b} - 2\hat{l}^*q_\pm^0 \pm \frac{\hat{b} + \hat{l}^*(2i\omega_0 + 4k^2)}{2q_+^0 - 1}\right] \pm \frac{i\omega_1}{2q_+^0 - 1}\,, \end{aligned} \quad (151)$$

apply. Substitution of these expansions into Eq. (146) determines the equation for the leading-order dispersion relation $\omega_0(k)$ to be $(2i\omega_0+\beta)(1-q_+^0)+i\omega(\beta-2\hat{b})$ which, after some manipulation, can be expressed as

$$4(i\omega_0)^3 + (i\omega_0)^2\left[4k^2 + 4\hat{b}(1-\hat{b}) + 2(1+2\hat{b})\beta - \beta^2\right] + 2i\omega_0\beta(\hat{b} + 2k^2) + \beta^2k^2 = 0\,. \quad (152)$$

This dispersion relation is identical to the result obtained when a constant density for the gas phase was assumed.[8] It is therefore concluded that in the absence of confinement and in the first approximation for small values of $\hat{r}$, the gas-phase thermal expansion has no effect on the stability behavior, a result that might be anticipated based on the small contribution of the mass fraction of gas in this limit.

The neutral stability boundary, corresponding to neither growth nor decay of the infinitesimal perturbations of the form given by Eqs. (140), can be displayed in a plane of the Zel'dovich number β, defined by the last of Eqs. (58), and the nondimensional wavenumber k. This boundary is obtained by setting the real part of the complex growth rate $i\omega$ to zero. By setting the real and imaginary parts of Eq. (152) separately to zero, the neutral stability boundary at leading order, $\beta_0(k)$, can be obtained as the positive root of the quadratic

$$(\hat{b}+2k^2)\beta_0^2+2\left[k^2-(1+2\hat{b})(\hat{b}+2k^2)\right]\beta_0-4(\hat{b}+2k^2)\left[\hat{b}(1-\hat{b})+k^2\right]=0\,, \tag{153}$$

and the corresponding leading-order frequency $\omega_0(k)$ of the neutral disturbance is

$$\omega_0^2=\frac{1}{2}\beta_0(\hat{b}+2k^2)\,. \tag{154}$$

Since $\omega_0 \neq 0$, the stability boundary is of the pulsating type, like that obtained for solid-propellant combustion in the absence of two-phase flow[17,20,21] (such intrinsic pulsating instabilities are also observable experimentally[27]). This leading-order stability boundary was obtained and discussed previously[8] and, for completeness, has been included in Fig. 7 (solid curves), which also exhibits the next-order approximation for a modified Zel'dovich number $\beta^0(k)$ (chain-dash and chain-dot curves) as discussed below. Several curves, corresponding to different values of $\hat{b}$, are shown, indicating that decreasing values of $\hat{b}$ are destabilizing, which suggests that diminished thermal influences of the gas phase (which convects heat away from the reaction zone in the direction of the burned region) is less able to damp the known thermal/diffusive instability of the condensed phase.[28] Indeed, we also show for reference the neutral stability boundary corresponding to strictly condensed-phase combustion (combustion synthesis), which can be recovered from the present analysis by setting $\hat{r}=\hat{l}=\hat{b}=1$ and $\alpha_s=0$ in Eq. (146). This stability boundary, which is determined (in the absence of melting) from the dispersion relation

$$4(i\omega)^3+(i\omega)^2\left[1+4k^2+2\beta-\frac{1}{4}\beta^2\right]+\frac{1}{2}(i\omega)(1+4k^2)+\frac{1}{4}\beta^2k^2=0\,, \tag{155}$$

is qualitatively similar to the stability boundaries obtained from (152), reflecting the fact that this particular type of instability phenomenon arises from combustion of the condensed phase, with the presence of the gas having a secondary, perturbative effect as discussed below. The fact that the minimum value of $\beta_0(k)$, given by $\beta_0=1+2\hat{b}+\sqrt{8\hat{b}}$, occurs at a nonzero value of $k=(\hat{b}/8)^{1/4}>0$ (as compared with $\beta_0=1+2\hat{b}+\sqrt{1+8\hat{b}}$ at $k=0$) suggests that nonplanar, cellular patterns will be observed at the transition to nonsteady burning as the stability boundary is crossed. Since the

leading-order results for the neutral stability boundary are independent of the porosity α_s, they are also the same as those obtained previously for a nonporous case in which two-phase-flow effects were confined to the liquid/gas region[14], as well as for a different model in which two-phase flow effects were suppressed in favor of an intrusive gas flame adjacent to a pyrolyzing solid surface.[20] Consequently, these same or very similar results are likely to occur in a variety of different energetic systems.

Since the leading-order results regarding the neutral stability boundary are independent of α_s, the leading-order effects of nonzero porosity are determined by proceeding to the next order with respect to the ratios of gas density and conductivity to those of the condensed phases. With the neutral stability boundary thus represented as

$$\beta \sim \beta_0 + \beta_1 \hat{r} + \cdots , \tag{156}$$

an expression for $\omega_1(k)$, introduced in Eq. (148), can be obtained from the dispersion relation at $O(\hat{r})$ given by

$$\begin{aligned} i\omega_1 \left[\beta_0 + 2(1-\hat{b}-q_+^0) - \frac{2i\omega_0+\beta_0}{2q_+^0-1}\right] + \frac{2i\omega_0}{\beta_0}(q_+^0 - 1 + \hat{b})\beta_1 = \frac{\alpha_s}{1-\alpha_s}\Bigg\{ \beta_0(1-q_+^0)\hat{l}^* \\ + \left[\frac{1}{2}\beta_0(2q_+^0-3) - i\omega_0(\beta_0-1) + \frac{i\omega_0\beta_0(q_+^0+1)}{i\omega_0+k^2}\right]\hat{b} + \frac{1}{2}\cdot\frac{2i\omega_0+\beta_0}{2q_+^0-1}\left[\hat{b} + (2i\omega_0+4k^2)\hat{l}^*\right]\Bigg\} \\ - \gamma_s^*\Bigg\{ (T_b^0-1)^{-1}\left[\beta_0(i\omega_0 - q_-^0) - \frac{q_+^0}{\hat{b}}(2i\omega_0+\beta_0)\right] \\ + (T_m-1)^{-1}(i\omega_0+q_-^0)(2i\omega_0+\beta_0)\, e^{(q_-^0-q_+^0)\ln[(T_b^0-1)/(T_m-1)]}\Bigg\}, \end{aligned} \tag{157}$$

where β_0 and ω_0 were given by Eqs. (153) and (154), respectively. It is observed that Eq. (157) differs from the corresponding result[8] that assumed a constant gas density, and thus modifications in the neutral stability boundary due to thermal expansion of the gas, as well as those due to two-phase flow, appear at this order in the analysis. Setting $\mathrm{Re}(i\omega_1)$ to zero and equating real and imaginary parts of Eq. (157) separately to zero then gives a coupled system of linear equations for β_1 and ω_1 that may be solved and analyzed.[9] These results are summarized below.

It can be shown that the $O(\hat{r})$ perturbation coefficient $\beta_1(k)$ with respect to the leading-order stability boundary $\beta_0(k)$ determined by Eq. (153) can be shown to consist of the sum of three contributions arising from the effects of nonzero density and thermal conductivity ratios $\hat{r}$ and $\hat{l}$, respectively, and the effects of a nonzero heat of melting. In particular,

$$\beta_1(k) = \frac{\alpha_s}{1-\alpha_s}\left[\hat{\beta}_r(k) + \hat{l}^*\hat{\beta}_l(k)\right] + \gamma_s^*\hat{\beta}_\gamma(k)\,, \tag{158}$$

where it is readily seen that for $\gamma_s^* = 0$, the solution for the perturbation coefficient β_1 is proportional to the factor $\alpha_s(1-\alpha_s)^{-1}$. Positive values of the coefficients $\hat{\beta}_r$, $\hat{\beta}_l$ and $\hat{\beta}_\gamma$ represent an upward, stabilizing shift in the neutral stability boundary from its leading-order position shown in

Fig. 2, while negative values represent a downward, destabilizing shift. The magnitude of these perturbations in the stability boundary, whether positive or negative, is seen from Eq. (158) to increase with increasing values of the porosity α_s. In addition, there is a wavenumber dependence for each effect, with nonzero values of $\hat{l}$ being destabilizing for small wavenumbers and stabilizing for large wavenumbers. The effect of nonzero values of $\hat{r}$, while generally destabilizing, exhibits the opposite trend (increasing destabilization for increasing wavenumbers), consistent with the physical expectation that the gas-to-solid/liquid thermal *diffusivity* ratio of the gas to that of the condensed phases, which is equal to $\hat{l}/\hat{b}\hat{r}$, should play a key role in determining the stabilizing or destabilizing influence of the gas phase.

For nonzero values of γ_s^*, the third component $\gamma_s^*\hat{\beta}_\gamma$ to the solution of β_1 provides a correction that is independent of α_s and, assuming an endothermic heat of melting ($\gamma_s^* < 0$), corresponds to the effect of increasing the amount of heat released in the reaction zone by the amount of heat absorbed by the liquid that accompanies the phase change in the preheat region. The effect of melting can be stabilizing or destabilizing,[8] although in the typical case of endothermic melting, the resulting correction in the stability boundary tends to be destabilizing, especially for smaller, more typical values of $\hat{b}$ and larger wavenumbers. This trend may be attributed to the fact that the release of the heat of melting by the liquid-to-gas reaction serves to enhance the heat release in the highly temperature-sensitive reaction zone, and that for $\hat{b} < 1$, a greater proportion of this energy is absorbed by the reactive condensed phase relative to that absorbed by the nonreactive gas. A similar destabilizing result was predicted for low-temperature melting in gasless systems,[29] although this effect diminishes and then reverses as the melting temperature increases such that melting occurs within the reaction zone itself.[28] Here, too, the effect of increasing T_m (while keeping T_b^0 and all other parameters fixed) is found to be stabilizing, particularly for small wavenumber disturbances.

There is a final $O(\hat{r})$ effect to be accounted for that is due to the change in the stability parameter β itself that accompanies any variation in the density ratio $\hat{r}$. Although we have thus far adhered to a conventional definition of the Zel'dovich number as defined by the last of Eqs. (58), this parameter itself varies with $\hat{r}$ through changes in the burned temperature T_b. In particular, for small values of $\hat{r}$, T_b decreases as $\hat{r}$ increases according to Eq. (149), thereby increasing the effective activation energy. Defining a modified Zel'dovich number β^0 that does not vary with $\hat{r}$ according to

$$\beta^0 = (1 - T_b^0)N^0\,, \quad N^0 \equiv \frac{\tilde{E}_l}{\tilde{R}\circ T_b^0}\,, \tag{159}$$

where T_b^0 is the leading-order burned temperature defined in Eq. (149), we calculate an additional correction $-\alpha_s(1-\alpha_s)^{-1}\hat{\beta}_1\hat{r}$ in the position of the neutral stability boundary with respect to the new parameter β^0, where $\hat{\beta}_1 = (1 - 2/T_b^0)\beta_0$, where $\beta_0(k)$ is the leading-order neutral stability boundary determined from Eq. (153). That is, analogous to Eqs. (156) and (158),

$$\beta^0 \sim \beta_0 + \left[\frac{\alpha_s}{1-\alpha_s}\left(\hat{\beta}_r + \hat{\beta}_l\hat{l}^* - \frac{T_b^0 - 2}{T_b^0}\beta_0\right) + \hat{\beta}_\gamma\gamma_s^*\right]\hat{r} + \cdots\,, \tag{160}$$

where $\hat{\beta}_r(k)$, $\hat{\beta}_l(k)$ and $\hat{\beta}_\gamma(k)$ are the same coefficients as those introduced in Eq. (158). The above two-term approximation of β^0 is shown in Fig. 7 (chain-dash curves) for the same values of $\hat{b}$ as the leading-order approximation β_0 and for typical values of the remaining parameters. Also shown in that figure are the corresponding (chain-dot) curves for the case of a constant gas-phase density,[8] which, while still indicating an overall destabilizing effect due to gas-phase influences, nonetheless lie above the modified stability boundaries that are obtained when thermal expansion of the gas is taken into account. However, because the constant-density analysis did not assume gas-phase quasi-steadiness, it can be argued[9] that at least part of this difference is likely attributable to the assumption of an instantaneous gas-phase response, since the latter may result in some overstatement of this destabilizing effect. From Eq. (160), it is clear that because the linearized correction to the leading-order result, due to nonzero values of the density and thermal conductivity ratios $\hat{r}$ and $\hat{l}$, is proportional to $\alpha_s(1-\alpha_s)^{-1}$, whereas the coefficient $\hat{\beta}_\gamma$ is independent of α_s, the effect of an increase in porosity is destabilizing with respect to steady, planar deflagration, and that this effect is enhanced by gas-phase thermal expansion.

IX. Conclusion

The present analysis has summarized recent advances in the application of multiphase-flow theory to the study of deflagrations in porous energetic materials such as degraded nitramine propellants. The focus in this work has been on the investigation of the effects of nonzero porosity and two-phase flow on the structure and stability of steady, planar deflagration. This was facilitated by the application of activation-energy asymptotics and the derivation of an appropriate asymptotic model for the general case of nonsteady, multidimensional propagation in both unconfined and confined materials. In the present work, this derivation proceeded under the assumption of a thermally expansive, quasi-steady gas phase, where the latter allowed the reduction of the more general confined problem to an analogous freely-propagting combustion wave with a specified pressure difference, or overpressure, between the burned and unburned states.

For the case of steady, planar propagation, it was demonstrated that the existence of an overpressure in the burned gas region has a significant effect on the burned temperature, gas-velocity profile, and the burning rate of the material. In particular, because of the pressure-driven permeation of the burned gases into the unburned material, a preheating effect is produced. Consequently, the temperature increases linearly, and hence the burning rate initially increases exponentially, with increases in the overpressure, followed by a more modest algebraic pressure dependence of the burning rate that is suggestive of Ap^n - type laws. This rapid increase in the burning rate, an explicit formula for which was derived, is in qualitative agreement with most experimental results on confined materials, which tend to show a sudden and rapid increase in the deflagration speed that is generally associated with the onset of convective burning. Thus, in contrast to the case of an unconfined deflagration, for which the gas flow relative to the condensed material is always in the downstream direction, the flow of gas in the unburned solid is, except in

the limit of small overpressures, always directed in the upstream direction, providing an important mechanism for preheating the unburned material and allowing the transition to a convection-enhanced mode of burning.

Since the steadily-propagating, planar combustion wave represents a basic solution of the more general nonsteady, nonplanar asymptotic model, its linear stability may be investigated in a reasonably straightforward fashion. This was illustrated for the case of an unconfined (constant pressure) deflagration, for which it was determined, as in previous studies of nonporous propellants and condensed-phase combustion, that a pulsating stability boundary exists in the plane of activation energy and disturbance wavenumber. The neutral stability boundary was shown to be especially accessible for realistic parameter values that furthermore permit the effects of porosity on the location of this stability boundary to be handled in a perturbative fashion. Specifically, in the realistic limit of small gas-to-solid/liquid density and thermal conductivity ratios, it was shown that shifts in the stability boundary were essentially proportional to $\alpha_s(1-\alpha_s)^{-1}$ and that the effects of thermal expansion and two-phase flow thus results in a destabilizing shift in the neutral stability boundary relative to the nonporous case. Additional stability results are under investigation for the confined geometry, where two-phase-flow effects associated with burned-gas permeation and the subsequent convective preheating of the material are anticipated to have an even more pronounced effect on the stability of the deflagration wave.

Acknowledgement

The work of the first author (SBM) was supported by the U. S. Department of Energy under Contract DE-AC04-94AL85000.

References

1. Kuo, K. K., and Summerfield, M., "Theory of Steady-State Burning of Gas-Permeable Propellants," *AIAA Journal*, Vol. 12, 1974, pp. 49–56.
2. Ermolayev, B. S., Borisov, A. A., and Khasainov, B. A., "Comments on 'Theory of Steady-State Burning of Gas-Permeable Propellants,' " *AIAA Journal*, Vol. 13, 1975, p. 1128.
3. Gokhale, S. S., and Krier, H., "Modeling of Unsteady Two-Phase Reactive Flow in Porous Beds of Propellant," *Progress in Energy and Combustion Science*, Vol. 8, 1982, pp. 1–39.
4. Margolis, S. B., Williams, F. A. and Armstrong, R. C. "Influences of Two-Phase Flow in the Deflagration of Homogeneous Solids," *Combustion and Flame*, Vol. 67, 1987, pp. 249–258.
5. Li, S. C., Williams, F. A., and Margolis, S. B., "Effects of Two-Phase Flow in a Model for Nitramine Deflagration," *Combustion and Flame*, Vol. 80, 1990, pp. 329–349.
6. Asay, B. W., Son, S. F., and Bdzil, J. B., "The Role of Gas Permeation in Convective Burning," *International Journal of Multiphase Flow*, Vol. 22, 1996, pp. 923–952.

7. Margolis, S. B., and Williams, F. A., "Effects of Two-Phase Flow on the Deflagration of Porous Energetic Materials," *Journal of Propulsion and Power*, Vol. 11, 1995, pp. 759–768.

8. Margolis, S. B., and Williams, F. A., "Influence of Porosity and Two-Phase Flow on Diffusional/Thermal Instability of a Deflagrating Energetic Material," *Combustion Science and Technology*, Vol. 106, 1995, pp. 41–68.

9. Margolis, S. B., and Williams, F. A., "Effect of Gas-Phase Thermal Expansion on Stability of Deflagrations in Porous Energetic Materials," *International Journal of Multiphase Flow*, Vol. 22, 1996, pp. 69–91.

10. Margolis, S. B., "A Deflagration Analysis of Porous Energetic Materials with Two-Phase Flow and a Multiphase Reaction Mechanism," *Journal of Engineering Mathematics*, Vol. 31, 1997, pp. 173–203.

11. Ilincic, N., and Margolis, S. B., "Eigenvalue Analysis and Calculations for the Deflagration of Porous Energetic Materials in the Merged-Flame Regime," *Combustion Science and Technology*, Vol. 125, pp. 201–241.

12. Margolis, S. B., "Influence of Pressure-Driven Gas Permeation on the Quasi-Steady Burning of Porous Energetic Materials," *Combustion Theory and Modelling*, Vol. 2, pp. 95–113.

13. Baer, M. R. and Nunziato, J. W., "A Two-Phase Mixture Theory for the Deflagration-to-Detonation Transition (DDT) in Reactive Granular Materials," *International Journal of Multiphase Flow*, Vol. 12, 1986, pp. 861–889.

14. Margolis, S. B., and Williams, F. A., "Stability of Homogeneous-Solid Deflagration with Two-Phase Flow in the Reaction Zone," *Combustion and Flame* Vol. 79, 1990, pp. 199–213.

15. Baer, M. R., and Shepherd, J. E., "A Thin Flame Model for Reactive Flow in Porous Materials," Sandia National Laboratories, SAND83–2576, Albuquerque, NM, 1984.

16. Mitani, T., and Williams, F. A., "A Model for the Deflagration of Nitramines," *Twenty-First Symposium (International) on Combustion*, The Combustion Institute, Pittsburgh, PA, pp. 1965–1974.

17. Denison, M. R., and Baum, E., "A Simplified Model of Unstable Burning in Solid Propellants," *ARS Journal*, Vol. 31, 1961, pp. 1112–1122.

18. Krier, H., T'ien, J. S., Sirignano, W. A., and Summerfield, M., "Nonsteady Burning Phenomena of Solid Propellants: Theory and Experiments," *AIAA Journal*, Vol. 6, 1968, p. 278.

19. De Luca, L., "Nonlinear Stability Theory of Heterogeneous Thin Flames," *Eighteenth Symposium (International) on Combustion*, The Combustion Institute, Pittsburgh, PA, 1981, pp. 1439–1450.

20. Margolis, S. B., and Armstrong, R. C., "Two Asymptotic Models For Solid Propellant Combustion," *Combustion Science and Technology*, Vol. 47, 1986, pp. 1–38.

21. Margolis, S. B., and Williams, F. A., "Diffusional/Thermal Coupling and Intrinsic Instability

of Solid Propellant Combustion," *Combustion Science and Technology*, Vol. 59, 1988, pp. 27–84.

22. Margolis, S. B., and Williams, F. A., "Diffusional/Thermal Instability of a Solid Propellant Flame," *SIAM Journal on Applied Mathematics*, Vol. 49, 1989, pp. 1390–1420.
23. Higuera, F. J., and Liñán, A., "Stability of Solid Propellant Combustion Subject to Nonplanar Perturbations," *Dynamics of Flames and Reactive Systems*, Vol. 95, Progress in Astronautics and Aeronautics, AIAA, New York, 1984, pp. 248–256.
24. Taylor, J. W., "The Burning of Secondary Explosive Powders by a Convective Mechanism," *Transactions of the Faraday Society*, Vol. 58, 1962, p. 561.
25. Boggs, T. L., "The Thermal Behavior of Cyclotrimethylenetrinitramine (RDX) and Cyclotetramethylenetetranitramine (HMX)," edited by K. K. Kuo and M. Summerfield, Vol. 90, Progress in Astronautics and Aeronautics, AIAA, New York, 1984, pp. 121–175.
26. Probstein, R. F., *Physicochemical Hydrodynamics*, Butterworths, Boston, 1989, pp. 98–100.
27. Zanotti, C., Carretta, U., Grimaldi, C., and Colombo, G., "Self-Sustained Oscillatory Burning of Solid Propellants," *Nonsteady Burning and Combustion Stability of Solid Propellants*, edited by L. De Luca, E. W. Price and M. Summerfield, Vol. 143, Progress in Astronautics and Aeronautics, AIAA, Washington, DC, 1992, pp. 399–439.
28. Margolis, S. B., "The Transition to Nonsteady Deflagration in Gasless Combustion," *Progress in Energy and Combustion Science*, Vol. 17, pp. 135–162.
29. Aldushin, A. P., Vol'pert, V. A., and Filipenko, V. P., "Effect of Reagent Melting on Combustion Stability for Gasless Systems," *Combustion, Explosion, and Shock Waves*, Vol. 23, 1987, pp. 408–414.

Figure Captions

Fig. 1. Schematic illustration of deflagration in porous energetic material with two-phase flow in both the solid/gas and liquid/gas regions, with combustion occurring in the latter. In the general case of a confined or partially confined geometry, a difference between the upstream (unburned) and downstream (burned) values of the gas pressure drives a portion of the burned gases into the pores of the unburned solid, as shown. In the unconfined limit of small overpressures ($p_g^b \to 1$), the gas flow is everywhere in the downstream direction, whereas for sufficiently large overpressures, even the gas flow in the burned region is directed upstream.

Fig. 2. Final burned temperature T_b as a function of the overpressure $p_g^b - 1$. As the overpressure increases past a critical value, T_b changes from a decreasing to an increasing function of the porosity α_s.

Fig. 3. Burned gas velocity u_g^b as a function of the overpressure $p_g^b - 1$. Also shown is the gas velocity $u_g(0)$ at the solid/liquid interface. Negative values indicate gas flow in the upstream direction, toward the unburned solid.

Fig. 4. Normalized burning-rate coefficient U_n as a function of the overpressure $p_g^b - 1$.

Fig. 5. Pressure profile $p(\xi)$ in the gas-permeation region for O(1) overpressures. Also shown is the velocity profile $u_g(\xi)$.

Fig. 6. Scaled pressure profile $P(\xi)$ in the gas-permeation region for large overpressures.

Fig. 7. Leading-order neutral stability boundaries $\beta_0(k)$ (solid curves) for the unconfined problem as a function of wavenumber for several values of the gas-to-liquid/solid heat-capacity ratio $\hat{b}$. Also shown is the corresponding neutral stability boundary (top curve) for the strictly solid combustion-synthesis (SHS) problem, and the modified boundaries $\beta^0(k)$ (chain-dot and chain-dash curves for constant and nonconstant gas density, respectively) that are obtained when the next-order correction with respect to $\hat{r}$ is included. The latter boundaries are calculated for reasonable values of the remaining parameters ($\alpha_s = 0.3$, $\gamma_s = 0$, $\hat{r} = 0.1$, $\hat{l}^* = 1.0$, $T_b^0 = 6.0$).

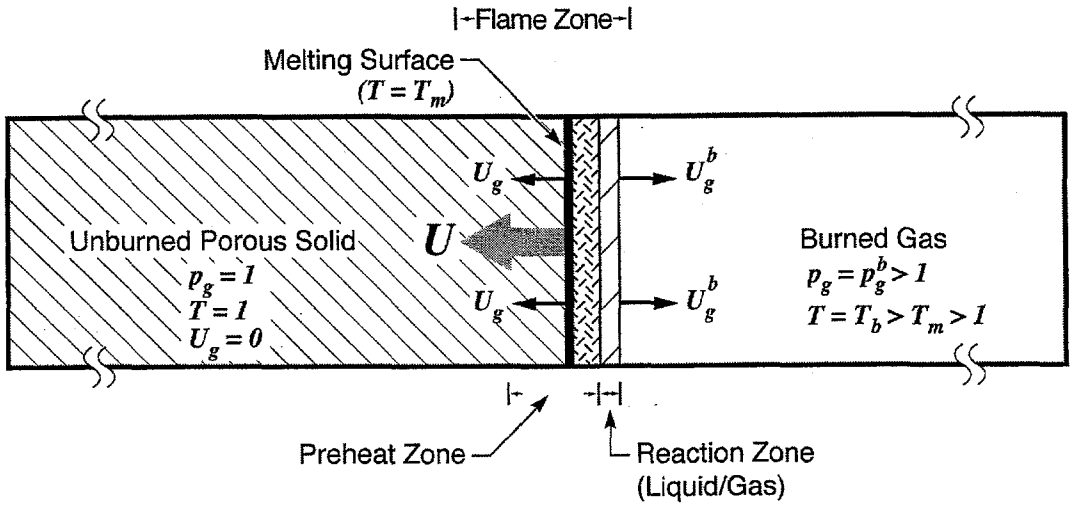

Figure 1

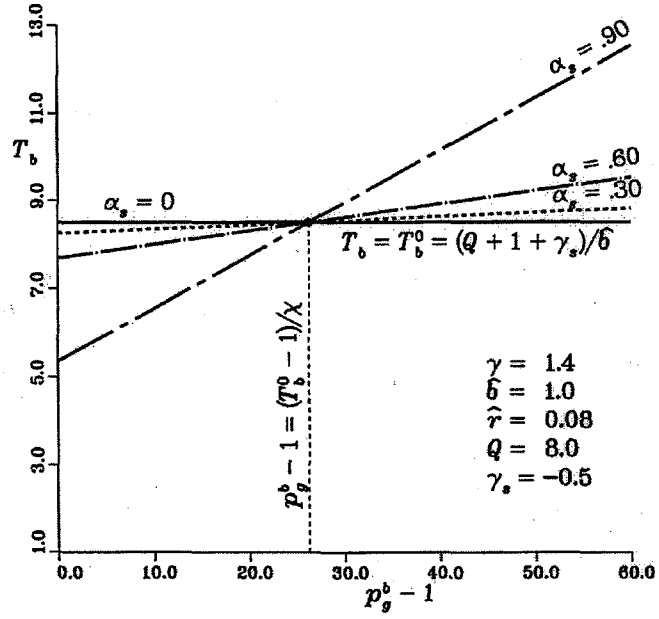

Figure 2

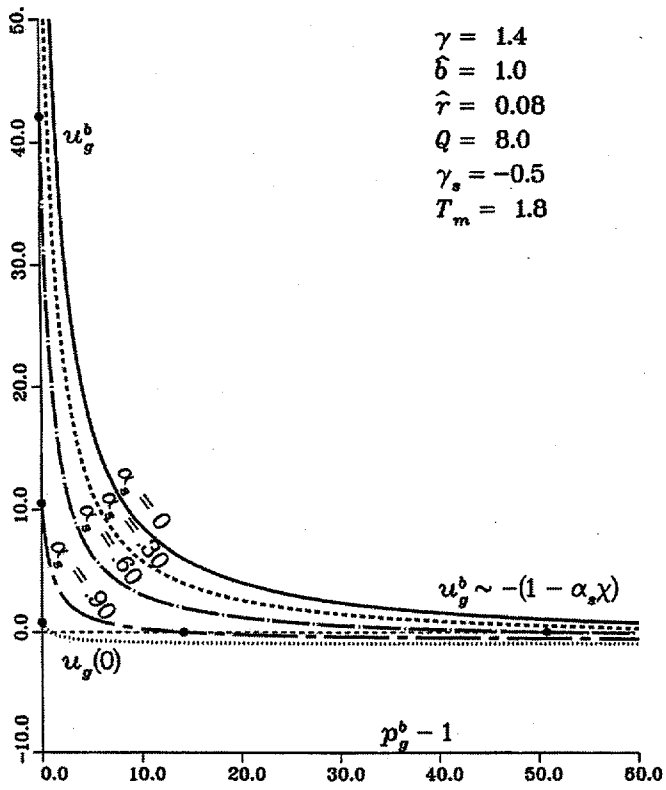

Figure 3

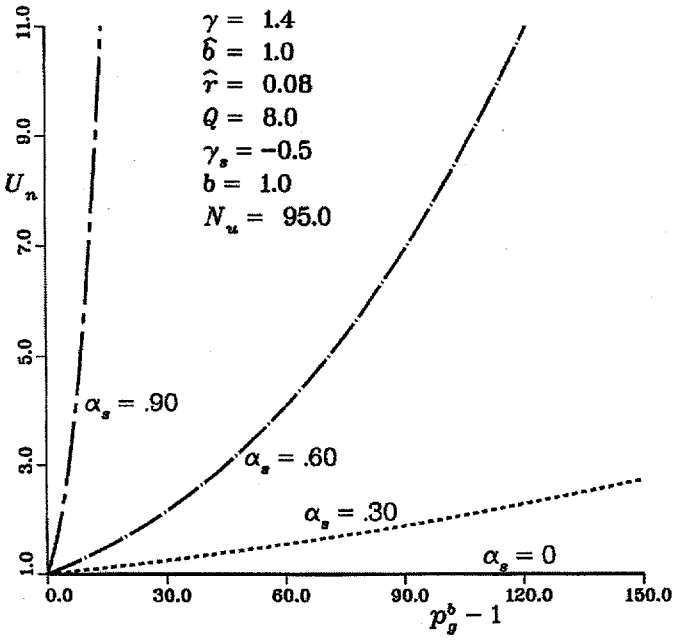

Figure 4

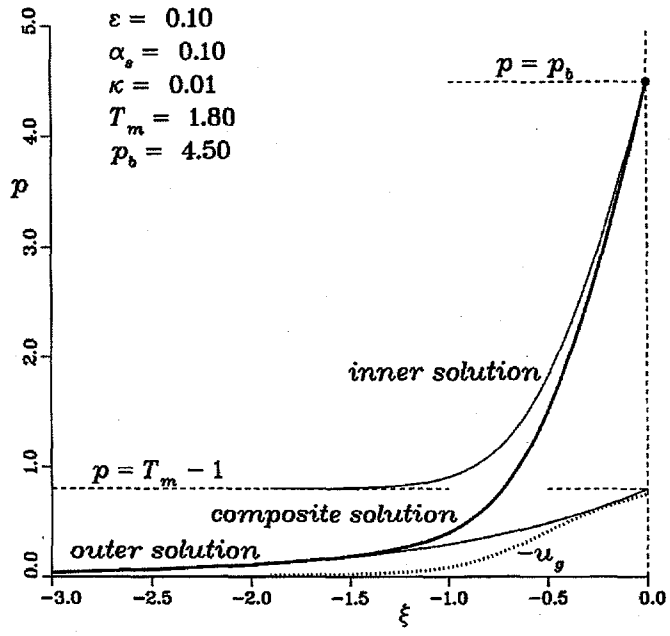

Figure 5

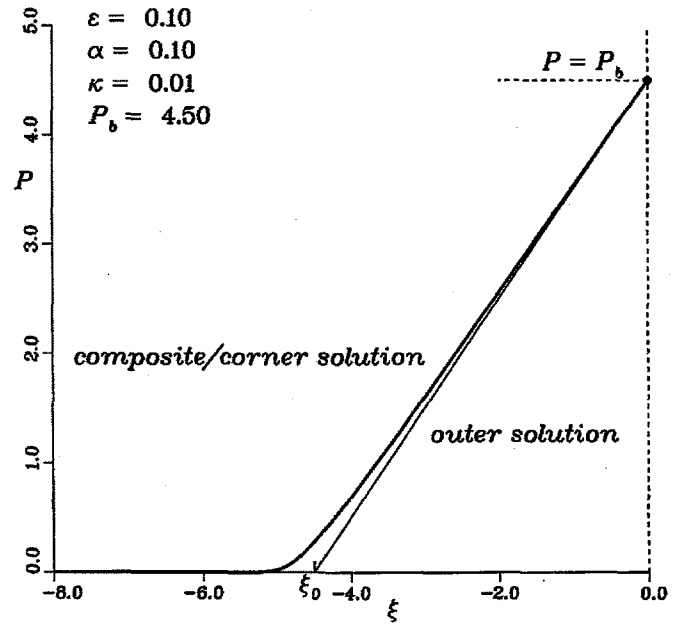

Figure 6

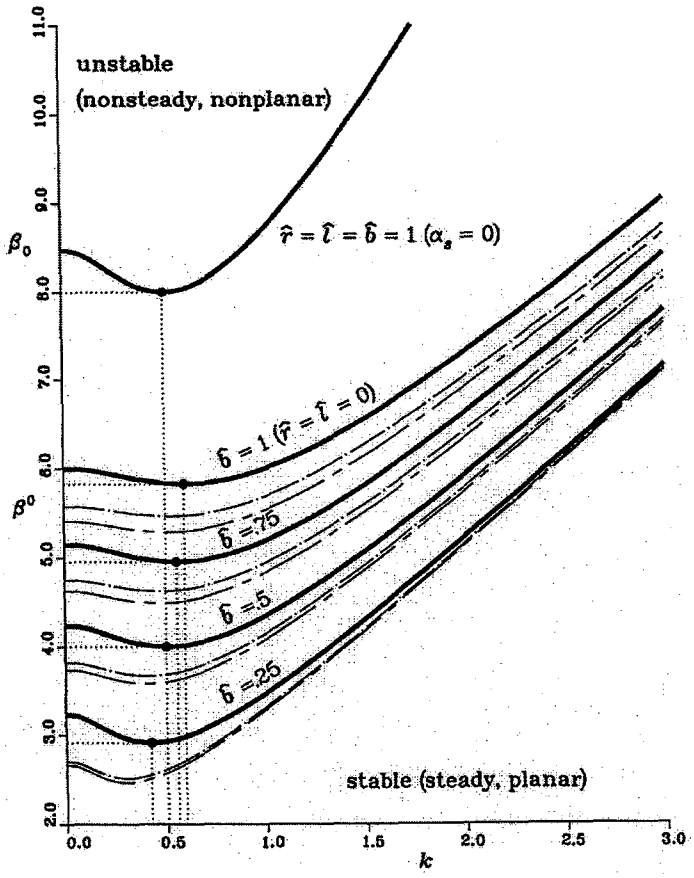
unstable
(nonsteady, nonplanar)
$\hat{\tau} = \hat{\iota} = \hat{\delta} = 1\ (\alpha_s = 0)$
$\hat{\delta} = 1\ (\hat{\tau} = \hat{\iota} = 0)$
$\hat{\delta} = .75$
$\hat{\delta} = .5$
$\hat{\delta} = .25$
stable (steady, planar)
β_0
β^0
k
11.0
10.0
9.0
8.0
7.0
6.0
5.0
4.0
3.0
2.0
0.0
0.5
1.0
1.5
2.0
2.5
3.0

Figure 7

UNLIMITED RELEASE

INITIAL DISTRIBUTION

Dr. John K. Bechtold
Department of Mathematics
New Jersey Institute of Technology
Newark, NJ 07102-1982

Dr. Mitat A. Birkan
Program Manager
Directorate of Aerospace and Engineering Sciences
Department of the Air Force
Bolling Air Force Base, DC 20332-6448

Prof. Michael Booty
Department of Mathematics
New Jersey Institute of Technology
Newark, NJ 07102-1982

Prof. John D. Buckmaster
Department of Aeronautical and Astronautical Engineering
University of Illinois
Urbana, IL 61801

Prof. Sebastien Candel
Ecole Central des Arts et Manufactures
Grande Voie de Vignes
92290 Chatenay-Malabry
FRANCE

Dr. John Card
Department of Mechanical Engineering
Yale University
New Haven, CT 06520

Prof. J. F. Clarke
College of Aeronautics
Cranfield Institute of Technology
Cranfield-Bedford MK43 OAL
ENGLAND

Prof. Paul Clavin
Laboratoire Dynamique et Thermophysique des Fluides
Universite de Provence
Centre Saint Jerome
13397 Marseille Cedex 4
FRANCE

Prof. F. E. C. Culick
Jet Propulsion Center
California Institute of Technology
Pasadena, CA 91125

Prof. Martin Golubitsky
Department of Mathematics
University of Houston
University Park
Houston, TX 77004

Prof. Michael Gorman
Department of Physics
University of Houston
Houston, TX 77004

Dr. Daryl D. Holm
CNLS, MS 457
Los Alamos National Laboratory
Los Alamos, NM 87545

Prof. G. M. Homsy
Department of Chemical Engineering
Stanford University
Stanford, CA 94305

Dr. G. Joulin
Laboratoirie D'Energetique et de Detonique
Universite de Poitiers
Rue Guillaume VII
86034 Poitiers
FRANCE

Dr. Hans Kaper
Applied Mathematics Division
Argonne National Laboratory
9700 S. Cass Ave.
Argonne, IL 60439

Prof. A. K. Kapila
Department of Mathematical Sciences
Rensselaer Polytechnic Institute
Troy, NY 12128

Prof. D. R. Kassoy
Department of Mechanical Engineering
University of Colorado
Boulder, CO 80309

Prof. Joseph B. Keller
Department of Mathematics
Stanford University
Stanford, CA 94305

Prof. Barbara Keyfitz
Department of Mathematics
University of Houston
University Park
Houston, TX 77004

Prof. C. K. Law
Department of Mechanical and Aerospace Engineering
Engineering Quadrangle
Princeton University
Princeton, NJ 08544

Dr. Gary Leaf
Applied Mathematics Division
Argonne National Laboratory
9700 S. Cass Avenue
Argonne, IL 60439

Prof. Amable Liñán
Universidad Politecnica de Madrid
Escuela Tecnica Superior de Ingenieros Aeronauticos
Plaza del Cardenal Cisneros, 3
Madrid - 3
SPAIN

Prof. J. T. C. Liu
Division of Engineering, Box D
Brown University
Providence, RI 02912

Prof. Moshe Matalon
Department of Engineering Sciences and Applied Mathematics
Northwestern University
Evanston, IL 60208

Prof. Bernard J. Matkowsky
Department of Engineering Sciences and Applied Mathematics
Northwestern University
Evanston, IL 60208

Prof. A. C. McIntosh
Department of Fuel and Energy
University of Leeds
Leeds LS2 9JT
United Kingdom

Prof. D. O. Olagunju
Department of Mathematical Sciences
University of Delaware
Newark, DE 19716

Prof. R. E. O'Malley
Department of Applied Mathematics
University of Washington Seattle, WA 98195

Prof. Norbert Peters
Institute fur Allgemeine Mechanik
Technische Hochschule Aachen
Aachen
GERMANY

Prof. Victor Roytburd
Department of Mathematical Sciences
Rensselaer Polytechnic Institute
Troy, NY 12128

Prof. W. A. Sirignano
Office of the Dean
School of Engineering
University of California, Irvine
Irvine, CA 92717

Prof. L. Sirovich
Division of Applied Mathematics, Box F
Brown University
Providence, RI 02912

Prof. G. I. Sivashinsky
Department of Mathematics
Tel-Aviv University
Ramat-Aviv, Tel-Aviv 69978
ISRAEL

Prof. Mitchell D. Smooke
Department of Mechanical Engineering
Yale University
New Haven, CT 06520

Prof. D. Scott Stewart
Department of Theoretical and Applied Mechanics
University of Illinois
Urbana, IL 61801

Prof. C. H. Su
Division of Applied Mathematics, Box F
Brown University
Providence, RI 02912

Prof. Cesar Treviño
Departmento de Termica y Fluidos
Universidad Nacional Autonoma de Mexico
Facultad de Ingenieria
Patios No. 12, Jardines del Sur
MEXICO 23, D.F.

Prof. Vladimir Volpert
Department of Engineering Sciences and Applied Mathematics
Northwestern University
Evanston, IL 60208

Dr. David Weaver
Air Force Rocket Propulsion Laboratory
DYP/Stop 24
Edwards Air Force Base, CA 93523

Prof. Forman A. Williams
Department of Applied Mechanics and Engineering Sciences
University of California, San Diego
La Jolla, CA 92093

Prof. Vigor Yang
Department of Mechanical Engineering
Pennsylvania State University
University Park, PA 16802

Prof. Benn Zinn
Department of Aerospace Engineering
Georgia Institute of Technology
225 North Avenue, NW
Atlanta, GA 30332

C. K. Westbrook, LLNL, L-321

MS 1110 R. C. Allen, 1422
MS 0834 A. C. Ratzel, 9112
MS 0834 M. R. Baer, 9112
MS 0834 M. L. Hobbs, 9112
MS 0834 R. J. Gross, 9112

MS 9001 T. O. Hunter, 8000
MS 9405 R. E. Stoltz, 8008
MS 9004 M. E. John, 8100
MS 9213 S. C. Johnston, 8103
MS 9054 W. J. McLean, 8300
MS 9163 W. Bauer, 8302
MS 9042 C. M. Hartwig, 8345
MS 9056 L. A. Rahn, 8351
MS 9051 W. T. Ashurst, 8351
MS 9051 A. R. Kerstein, 8351
MS 9052 D. R. Hardesty, 8361
MS 9055 R. Behrens, 8361
MS 9052 S. B. Margolis, 8361 (30)
MS 9053 R. W. Carling, 8362
MS 9021 Technical Communications Department, 8815, for DOE/OSTI
MS 9021 Technical Communications Department, 8815/Technical Library, MS 0899, 4916
MS 0899 Technical Library, 4916
MS 9018 Central Technical Files, 8940-2 (3)